Acknowledgement

I am highly grateful to the authorities of Thapar Institute of Engineering and Technology, Patiala for providing me an opportunity to carry out the present thesis research work.

I express my deep sense of gratitude and thanks to my revered supervisors **Dr. S.K. Mohapatra**, Professor and Head of the Mechanical Engineering Department, TIET, Patiala and **Sh. V.K. Singla**, Lecturer, Mechanical Engineering Department, TIET, Patiala, for their sincere and invaluable guidance, suggestions and sympathetic attitude which inspired me to submit this thesis report in the present form.

I am also indebted to all the staff members of TIET and R and D centre, Patiala and my fallow students who were always there at the need of the hour and provided me the required help and facilities for the completion of my thesis.

I am also thankful to the authors whose research work I have consulted and quoted in this work. Last but not the least, I would like to thank God for not letting me down at the time of crisis and showing me the silver lining in the dark clouds.

(Deepak Kumar)

Table of Contents

Title **Page No.**

List of Figures

Figure No. **Title** **Page No.**

SEM pictures

List of Tables

Table No. **Title** **Page No.**

Abstract

Study on the research problem entitled "Experimental Investigation on Surface Modification with Powder Mixed Electric Discharge Machining" was conducted in the M.E.D., T.I.E.T., Patiala during the year 2006. Electrical discharge machining (EDM) is a manufacturing process by which tool cuts the required shape into the workpiece within a dielectric fluid. In the past, research has been done to develop and improve different models of the material removal from both tool and workpiece. Recently, a new process of surface modification by EDM process has been evolved by mixing some suitable material in powder form into the dielectric fluid of EDM for improving the life of metal. This new process is called Powder Mixed EDM (PMEDM). In the present investigation, two powders i.e. Aluminium oxide (Al_2O_3) and Silicon carbide (SiC) both @ 2, 8 and 16 g/l, were mixed in dielectric fluid with a view to study the effect of powders suspended into the dielectric fluid on the surface modification. Machining parameters viz., dielectric type, peak current, pulse duration, concentrations of powders, etc. were changed to explore their effects on machining performance as judged from the material removal rate (MRR), tool wear rate (TWR), surface roughness (SR), hardness and micro-structure. The surface roughness and hardness of workpiece were improved by optimizing various combinations of Al_2O_3 and SiC powders mixed in kerosene with different ratio. The combination of powders weighing112 g mixed in 7 litres of kerosene was found to be the best. The quality of machined surface was analyzed by using the scanning electron microscope (SEM). SR values of machined surface of each workpiece were measured using the surface roughness measuring instruments "perthometer" and "surf test". The use of powders was evaluated by recording observations on various input and output parameters. Addition of SiC powder @ 16 g/l into the dielectric was found to be the best as judged from its effects effect on various parameters. The same process also imparted the maximum hardness to the machined surface of the workpiece. It was further observed that MRR value was more in simple process as compared to Al_2O_3 and SiC processes. MRR was the maximum in straight polarity process as compared to reverse polarity process while TWR was higher in general but the highest in case of SiC when used at the concentration of 16 g/l.

Chapter-1
Introduction

1.1 Introduction

As technological advances are taking place in the field of space research, and missile and nuclear industry in the world; very complicated and precise components having some special requirements are demanded by these industries. New developments taking place in the manufacturing field to meet the new challenges. After World War II, many new materials and unconventional methods of forming difficult to machine metals have emerged which are being put to commercial use with time. The word unconventional is used in the sense that the metals like tungsten, hardened stainless steel, tantalum, some high strength steel alloys, etc., are such that they can't be machined by conventional methods but require some special techniques. The conventional methods are inadequate to machine such materials from stand point of economic production.

The unconventional methods of machining have several specific advantages over conventional methods of machining and these promise formidable tasks to be undertaken and set a new record in the manufacturing technology. These methods are not limited by hardness, toughness, and brittleness of the material and can produce any intricate shape on any workpiece material by suitable control over the various physical parameters of the processes. Non-traditional Manufacturing (NTM) processes can be broadly categorized according to: (1) processes in which there is a non-traditional mechanism of interaction between the tool and the workpiece, and (2) processes in which non-traditional media are used to affect the transfer of energy from the tool to the workpiece. In contrast, traditional machining relies on direct mechanical contact between the tool and the workpiece, which often causes undesired changes in the properties of workpiece, such as residual mechanical and thermal stresses. Rising production costs dictate that production operations be automated whenever possible; innovative materials such as super-alloys, composites, ceramics and many other advanced materials, which are difficult to or cannot be processed by traditional machining methods, require new manufacturing technologies; environmental considerations require the development of environmentally conscious processes. These engineering challenges facilitated the development of non-traditional

manufacturing processes. NTM processes are usually well suited to be monitored and controlled, the processing steps are reduced, the fixtures are simplified due to their inherent non-contact nature, and the process precision covers a wide range. In many cases, traditional manufacturing may have reached their capability limits, while NTM is offering the best solution. NTM is also expanding its applications to what has been dominated by conventional processes. For example, laser is widely accepted as an economical, high throughout tool for metal/ceramics cutting and drilling with thin to medium thickness. Engineering achievements in recent years, such as electronics industry, MEMS and Rapid Prototyping Manufacturing (RPM), are impossible without the development of critical NTM processes. Thermally based energy transfer is the main material removal mechanism for several non-traditional machining processes including electrical discharge machining, laser machining, electron beam machining, plasma arc cutting, etc.

Thermal phenomena are also central in processes such as laser forming, laser sintering, laser cladding and laser material deposition. In processes such as electrochemical machining, thermal field can strongly influence the chemical reaction rate. Despite the high intensity thermal field involved, many non-traditional machining processes have good control of the thermal effects during machining. For example, laser energy can be precisely controlled to produce high machining quality with a very narrow heat affected zone.

Water jet machining and electrochemical machining are inherently less liable to induce thermal damages to the target material. Thermal effects can be useful in some cases. For example, conventional machining can be extended to the machining of ceramics with the assistance of plasma or laser beam.

1.2 New Technological Processes

In non-conventional machining methods, there is no direct contact between the tool and the workpiece; hence the tool needs not be harder than the job. Further, in spite of the recent technical advancements, the conventional machining processes are inadequate to produce complex geometrical shapes in the hard and temperature resistant alloys and die steels. Keeping these requirements into mind, a number of non-conventional methods

have been developed. These new technological processes can be classified into various groups as given below:

Mechanical Processes

In mechanical processes, metal removal takes place either by the mechanism of simple shear or by erosion mechanism where high velocity particles are used as transfer media and pneumatic/hydraulic pressure acts as a source of energy. It includes ultrasonic machining (USM), water jet machining (WJM), abrasive jet machining (AJM), etc.

Thermal Processes

Thermal processes involve the application of very thin intense local heat. Here melting or vaporization from the small areas at the surface of the workpiece removes material. The source of energy used is amplified light, ionized material and high voltage. Examples are laser beam machining (LBM), ion beam machining (IBM), plasma arc machining (PAM), and electric discharge machining (EDM).

Electro-chemical Processes

Electro-chemical processes involve removal of metal by the mechanism of ion displacement. High current is required as the source of energy, and electrolyte acts as transfer media. It includes electro-chemical machining (ECM), electro-chemical grinding (ECG), etc.

Chemical Processes

Chemical processes involve the application of resistant material (acidic or alkaline in nature) to certain portion of the work surface. The desired amount of material is removed from the remaining area of the workpiece by the subsequent application of an etching that converts the workpiece material into a dissolvable metallic salt. It includes chemical machining (CHM) and photochemical machining (PCM).

1.3 Problem Formulation

Technological advances have led to an increasing use of material with high strength and hardness material in manufacturing industries. In the machining of the material, traditional manufacturing processes are increasingly being replaced by non-conventional machining techniques such as electro discharge machining (EDM), ultrasonic machining (USM), electro chemical machining (ECM) and laser beam

machining (LBM). EDM has found widespread applications in tool and mold industries, and aerospace industries. Therefore, promotion of the quality of the EDM process by developing a thorough understanding of the relationship between the EDM parameters and the machined surface integrity has become a major research concern.

In general, application of EDM is not constrained by the hardness or the material strength to be machined. EDM may be used to machine any conductive material. Another added advantage of EDM is that there is no direct contact between the tool and workpiece during machining and hence no deformation occurs even for thin components. However, due to the quick heating and cooling effects induced by machining process, a thermally affected layer will get deposited on the surface of the workpiece. The structure of this layer is quite different from the parent material. The defects such as voids, cracks, etc. cause an overall deterioration of mechanical properties of the workpiece.

In order to improve upon the efficiency and to modify the surface of the workpiece, some particles in the powder form are mixed into the dielectric fluid as a suspension at tool workpiece interface during machining. This new technique in EDM is named as Powder Mixed EDM (PMEDM).

In PMEDM, some metallic powders such as aluminium, silicon, nickel, etc. can be suspended into dielectric fluid. When suitable voltage is applied between both the electrodes through powder mixed dielectric fluid, the powder particles tend to gather around surface irregularities due to electric field concentration around such points. The added powder facilitates the bridging effect and minimizes the insulation strength of the dielectric fluid, thereby resulting in a discharge. The discharging period can effectively separate the discharging energy into several increments and facilitate in getting minimum size of debries and decreases surface roughness (SR) .Discharge will occur at a power voltage for the same spark gap; thus, the total time time spent in erosion is increased due to decrease in the lag time. As a result, an extremely corrosive resistant and micro-crack free uniform surface is produced. Enhanced effectiveness against corrosion is particularly needed for moulds and dies in which corrosive gases develop from plastic compounds. It is also found that the stability of machining is improved.

With these points in mind the present work was planned to identify the effect of relevant PMEDM operating parameters e.g. concentration of added powder, peak current,

pulse on time, pulse off time, electrode lift time, and nozzle flushing, etc. on surface roughness, surface hardness, and micro-structural changes in the base metal in order to achive enhanced surface integrity.

1.4 Objectives of Proposed Study

By reviewing the literature relevant to the proposed research problem, the following objectives of study were proposed:

1. To investigate the effect of addition of Al_2O_3 active neutral and SiC into the dielectric fluid of EDM on surface characteristics of the EN-24 workpiece.
2. To study the effect of powder added on MRR of both workpiece and tool.
3. To study the effect of the addition of powder on hardness of workpiece, and
4. To study microstructure of workpiece.

1.5 Work Justification

EDM machining technology is widely adopted in mechanical manufacturing. The EDM process is not affected by material hardness and strength. Its low efficiency and poor surface quality have been the key problems restricting its application. Therefore, it was considered to be of prime importance to improve the machining efficiency and surface quality of the EDM technology.

To overcome all these difficulties, the present study envisaged the development of new strategy called PMEDM process. The results produced by this process would be quite encouraging. The quality and integrity of the machined surface would be improved remarkably.

Chapter-2
Electric Discharge Machining

2.1 Introduction

Among all the non-conventional machining methods, EDM is one of the most popular machining methods in manufacturing of press tool and various dies. It is due to its capability to machine very hard material and the capability to produce complicated profiles. This process enables machining of any material, which is electrically conductive, in any shape, irrespective of its hardness or strength. Even highly delicate sections and weak materials can be machined without any fear of distortion because there is no direct contact between the tool and the workpiece. But its low efficiency and poor surface finish have been the key problems restricting its further development. Further, there is continues in the demand of modification of surfaces, development of heat and corrosion resistant work surface. Therefore it is of great importance to improve the machining efficiency and surface integrity of EDM technology.

A machining process, and more broadly, any manufacturing process, can be represented by the Process Conditions Scheme (PCS), which is the diagram used to analyze the condition features of machining and its conjugate (Figure. 2.1). The base side of the process condition triangle represents the kind of interactions such as thermal/electron beam (EB), plasma beam (PB), laser beam (LB) and electrical discharges (ED), electrochemical (EC), chemical (CH), and mechanical. Note that *A* denotes grinding and abrasive flow, *C* cutting (turning, milling, drilling etc), *US* ultrasonic wave, and *F* flow fluid action (high pressure water jet, low pressure suspension jet etc.). The left side of the triangle represents the set of energy carriers: Photons, Electrons, Ions, Plasma, Abrasives, Cutting edges, and Fluid jet. The right side of the triangle consists of types of working media: Solid particles, Electrolyte, Fluid, Dielectric and Gas.

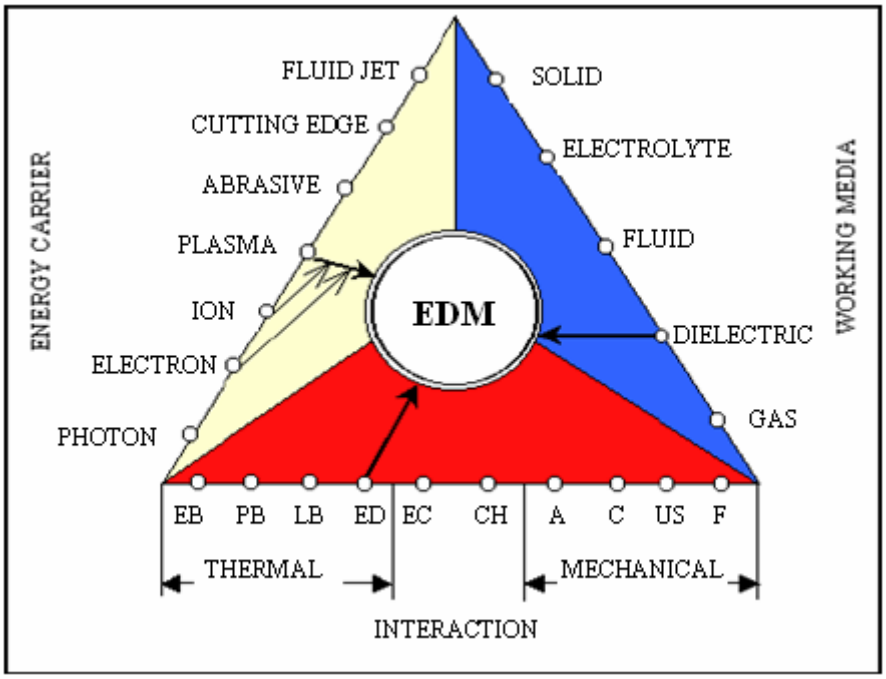

Figure 2.1: Process Conditions Scheme (PCS) for Electrical Discharge Machining

Recently, one of relative new methods of surface modification to improve the life of the material is evolved by EDM process by mixing some suitable material in powder form into the dielectric fluid of EDM (Figure 2.2). This process is termed as Powder Mixed EDM (PMEDM). It is reported that there is deposition of layer in the powder mixed EDMed surface, which has hard surface than the base metal, smaller surface roughness (SR), and high resistance to corrosion and abrasion. The results produced by this process in terms of process characteristics such as material removal rate (MRR), surface roughness (SR) and tool wear rate (TWR) are quite encouraging. The quality of the machined surface is improved considerably. However, little research work has been carried out to study PMEDM process. The role of the powder in PMEDM is very much complicated and its machining mechanism is still not clear. Efforts are going on to develop the well established theory behind the mechanism of PMEDM.

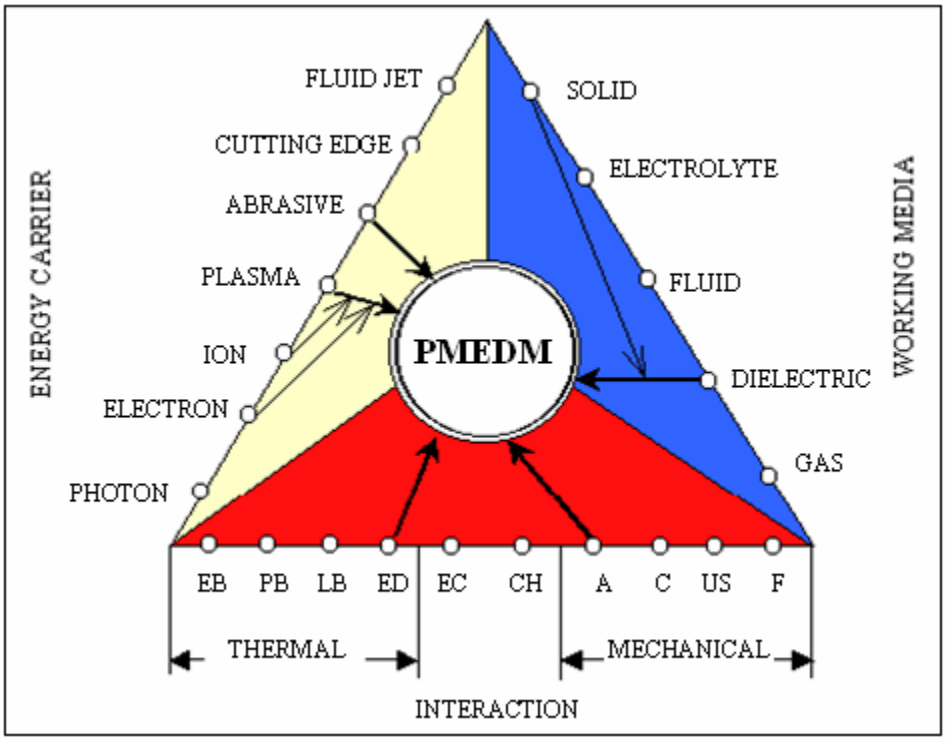

Figure 2.2: Powder Mixed Electrical Discharge Machining (PMEDM)

2.2 History of Electric Discharge Machining

Among all the non-conventional machining methods, EDM is one of the most popular machining methods in manufacturing of tools and dies. In 1970, the English scientist, Priestley, first detected the erosive effect of electrical discharges on metals. More recently, during their research, the Soviet scientists, Lazarenko and Lazarenko, decided to exploit the destructive effect of an electrical discharge and develop a controlled method of metal machining. In 1943, they announced the construction of the first spark erosion machine. The spark generator used in 1943, known as Lazarenko circuit, has been employed over many years in power supplies for EDM machines and an improved form is being used in many current applications. In EDM process, electric energy is used directly to cut the material to final shape and size. Efforts are made to utilize the whole energy by applying it at the exact spot where the operation is to be carried out. In this method, no complicated fixtures are needed for holding the job and even very thin jobs can be machined to the desired dimensions and shape. All the operations are carried out

in a single set-up. The process may be applied to machine steels, super alloys, refractoriness etc.

The popularity of EDM process is due to the following advantages:

- The process can be readily applied to electrically conductive materials. Physical and metallurgical properties of the work material, such as strength, toughness, microstructure, etc., are no barrier to its application.
- During machining, the workpiece is not subjected to mechanical deformation as there is no physical contact between the tool and work. This makes the process more versatile. As a result, slender and fragile jobs can be machined conveniently.
- Although the metal removal in this case is due to thermal effects, yet there is no heating in the bulk of the material.
- Complicated die contours in hard materials can be produced to a high degree of accuracy and surface finish.
- The overall production rate compares well with the conventional processes because it can dispense with operations like grinding, etc.
- The surface produced by EDM consists of a multitude of small craters. This may help in oil retention and better lubrication, especially for components where lubrication is a problem. The random distribution of the craters does not result in an appreciable reduction in fatigue strength of the components machined by EDM.
- The process can be automated easily thereby requiring very little attention from the machine operator.

2.3 EDM Description

EDM has C type of construction. Its main components (Figure 2.3) are given as under:

1. Control Unit
2. Electrode holder
3. Electrode feed mechanism
4. Tank
5. Fixture

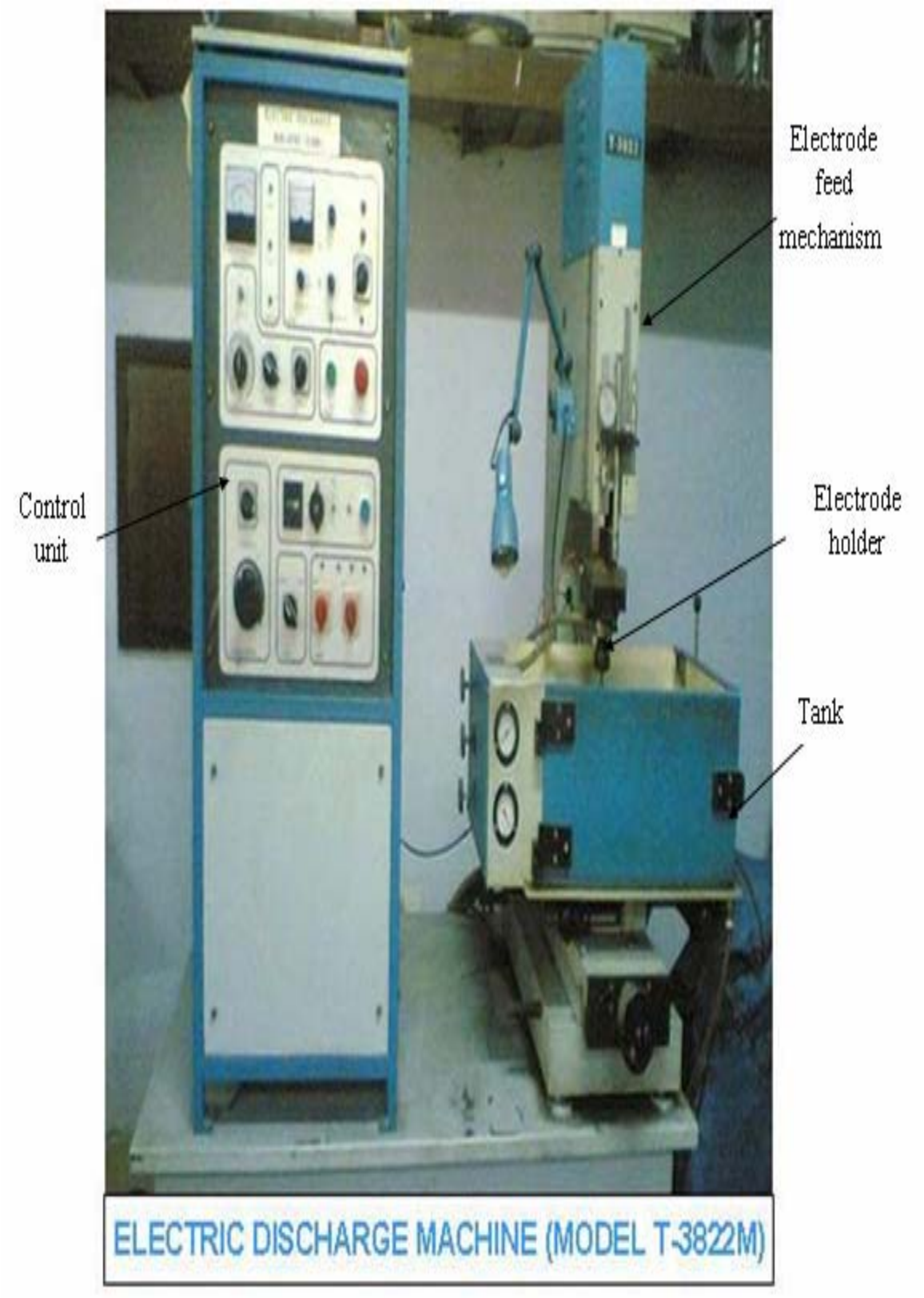

Figure 2.3: Showing Electric Discharge Machine (Model T – 3822M)

2.4 Description of EDM Controls

1. The controls of EDM (Model T- 3822M) are listed below:
2. Rotary Switch (Mains)
3. Indicator Lamps (Three Phase)
4. Rotary Switch (Finish)
5. Rotary Switch (Pump)
6. Rotary Switch (Current Range)
7. Rotary Knob (Current Adjust)
8. Ammeter (Gap Current)
9. Rotary Switch (Base)
10. Rotary Switch (Duration)
11. Indicator (Gap)
12. Rotary Potentiometer (Gap Control)
13. Toggle Switch (Soft Pulse)
14. Indicator Lamp (Spark)
15. Push Button (Spark)
16. Toggle Switch (Autoflushing)
17. Rotary Potentiometer (Sparking Time)
18. Rotary Potentiometer (Lifting Time)
19. Indicator Lamp (OV/SP)
20. Push Button Red (OFF)
21. Rotary Switch (AUT/MAN)
22. Push Button (UP/DN)
23. Indicator Lamp (Interlock)
24. Rotary Switch (Ignition)
25. Indicator Lamp (Pump ON)
26. Push Button (AUTOPOS)
27. Indicator Lamp (AUTOPOS)
28. Piezo Ceramic Alarm (Buzzer)
29. Toggle Switch (Buzzer Select)
30. Decade Counter (Hour Counter)

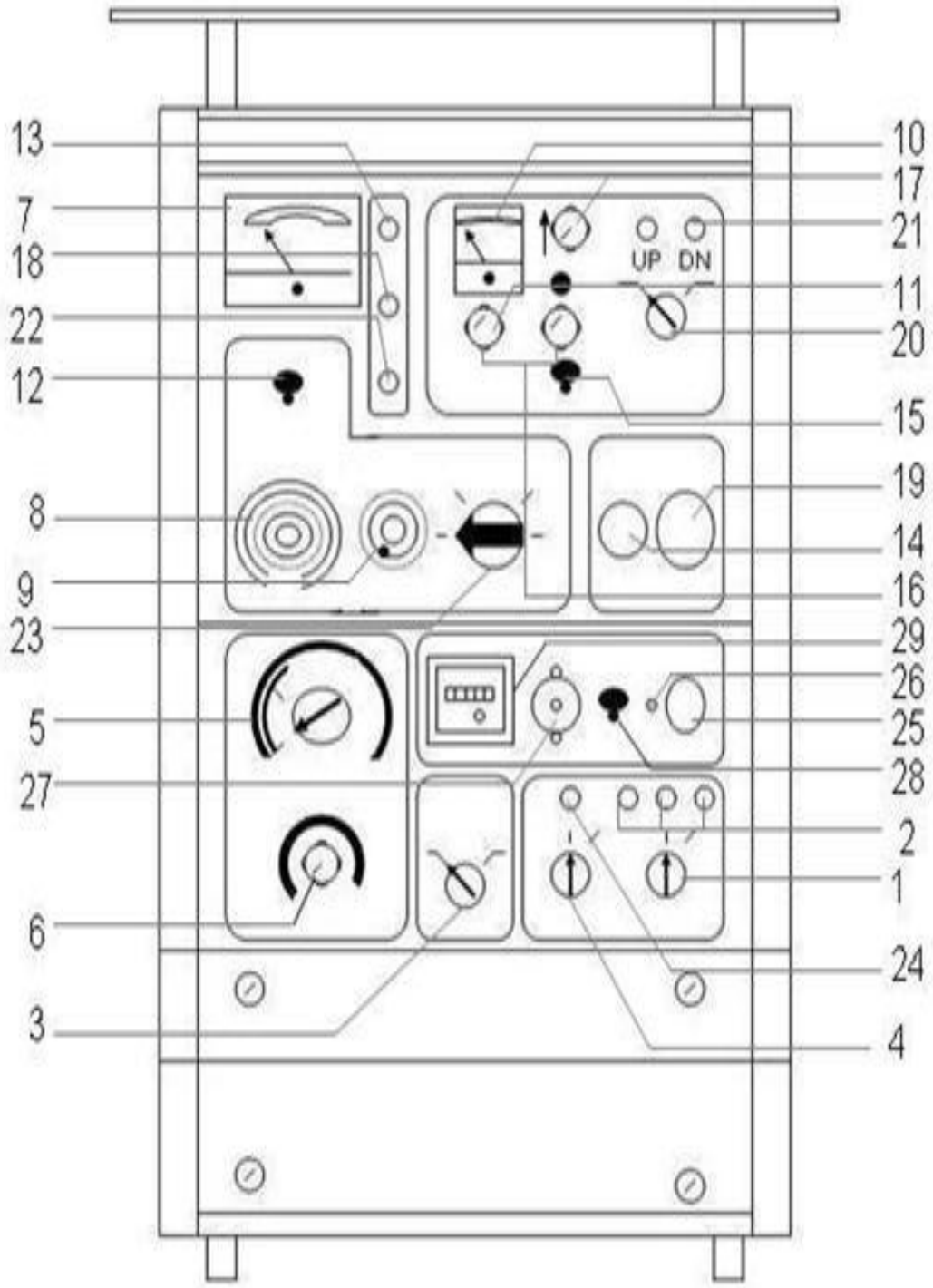

Figure 2.4: Indicating the controls of EDM (Model No. T – 3822M)

Various types of controls of EDM (Model T- 3822M) are explained as under:

Rotary Switch (Mains)

This is mains ON switch for total power supply (Generator). In position '1' the supply is ON and in position '0' the supply is OFF.

Indicator Lamps (Three Phase)

There are three LEDs (Light Emitting Diodes) indicating presence of three phases of main supply.

Rotary Switch (Finish)

This has two positions viz. NORMAL and MIRROR. The position MIRROR is selected only while polishing the job, for all other setting, electrode and workpiece material combinations, the NORMAL position is to be selected.

Rotary Switch (Pump)

This switch has two positions '0' and '1'. In position '1' the dielectric pump is started. In position '0' the pump is put OFF.

Rotary Switch (Current Range)

This switch has three positions. The positions '1' through '3' increase machining current in steps of 4 amperes.

Rotary Knob (Current Adjust)

This knob continuously adjusts machining current in the span of about four amperes. In range '1' the current varies from 0.2 to 4 amperes approximately. Current is minimum when the knob in fully counterclockwise (CCW) position and goes on increasing as the knob is turned in clockwise (CW) direction.

Ammeter (Gap Current)

This is a moving coil type ammeter indicating average machining current during the machining process. The range provided is 0 to 15 amps. Green band is upto 12 amps and the remaining is red band.

Rotary Switch (Base)

This switch has 8 positions which are explained as given below:

Positions 8, 7	-	Roughing
Positions 7, 6, 5, 4	-	Semi-finishing

Positions 5, 4, 3, 2 - Finishing

Position 1 - Super-finishing

To achieve good machining stability, the following ranges of machining current are recommended for different positions of rotary switch, as given in Table 2.1.

Base Position	Machining Current Range
8	06 A to 12 A
7	04 A to 12 A
6	03 A to 10 A
5	01 A to 08 A
4	0.5 A to 06 A
3	0.5 A to 04 A
2	0.1 A to 02 A
1	0.1 A to 01 A

Table 2.1: Ranges of machining current with respect to switch '8' (Base)

Rotary Switch (Duration)

This switch has '12' positions. The pulse duration can be changed from minimum (position 1) to maximum (position '12') in '12' positions by switch '9' (Duration) for each position of switch '8' (Base). Thus, one can obtain a full range of pulse duration from a minimum of 2 μs to a maximum of 520 μs which largely covers the duration limits used in a pulse generator with a total power of 3 KVA. Increasing the duration reduces the machining rate with a drastic reduction in the relative electrode tool wear.

Too long pulse duration (duration position '10' to '12') with copper electrode and steel workpiece results in excessive accumulation of carbon in the machining zone with a subsequent instability of the machining process.

Indicator (Gap)

Under healthy machining condition, the deflection is 1 to 1.5 divisions of its scale.

Rotary Potentiometer (Gap Control)

This control adjusts the servo to change deflection of indicator '10' (Gap). In CCW direction, the deflection goes on decreasing and vice versa.

Toggle Switch (Soft Pulse)

The function of this switch, when in position '1', is to smooth the discharge pulses which are very strong when the machining current is more than 2-3 amps. The purpose of this switch is to reduce arcing tendency and ensure stable machining process under these conditions.

Normally, Soft Pulse should be switched on (position '1') whenever the average machining current is greater than 2-3 amps. However, in finishing ranges where the machining current is less than 2-3 amps; putting off this switch improves the surface finish and also reduces the electrode-tool wear.

Indicator Lamp (Spark)

This LED is ON when machining starts. It is turned OFF momentarily during lifting period of auto flush cycle or when the machining gap is short.

Push Button (Spark)

Pressing of this push button (with indicator '18' and '22' OFF) starts the machining process.

Toggle Switch (Autoflushing)

This switch selects autoflushing (lifting during machining) in position '1'. In position '0' the autoflushing cycle stops.

Rotary Potentiometer (Sparking Time)

This control adjusts lifting time with Toggle Switch '15' (autoflushing) selecting. In CW direction, the sparking time goes on increasing.

Rotary Potentiometer (Lifting Time)

This control adjusts lifting time with Toggle switch '15' (autoflushing) selected. In CW direction, the time goes on increasing.

Indicator Lamp (OV/SP)

This LED is ON under single phasing condition or over voltage condition of main input i.e. when the voltage of one or more of the 3 phase mains input is above or below the safe working limits.

Push Button Red (OFF)

The machining (sparking) or auto position function can be stopped by pressing this push button.

Rotary Switch (AUT/MAN)

This switch selects one of the two modes of operation- automatic and manual. In position 'AUT', either sparking or autopositioning can be started. In position 'MAN', the manual up and down movement of the quill is possible.

Push Button (UP/DN)

This switch has center off position. This switch is effective in 'MAN' position of switch (20), with UP and DN position of the switch, upward and downward movement of quill is possible respectively.

Indicator Lamp (Interlock)

The LED is ON when level of dielectric is low in the working tank and causes interruption in the machining operation.

Rotary Switch (Ignition)

This is a 4-position switch. It controls the energy of ignition of discharge channel. This energy is maximum in position '1' of this switch and it decreases progressively as the switch is rotated from position '1' to '4'. Excessive ignition of the discharge channel provokes arcing tendency and instability of the machining process. Hence, whenever, the arcing tendency is more or the panel meter GAP (in spite of adjusting the GAP Control) is overshooting frequently, a higher position of switch ignition should be selected.

Current Range (amps)	Duration Range			
	1 - 3	4 – 5	6 – 8	9 - 12
6	2	3	4	4
2 – 6	2	3	¾	4
2	1/2	2/3	¾	4

Table 2.2. Indicating ignition positions for different durations and current ranges.

The position of rotary switch Base should be selected appropriate to the machining current range.

Indicator Lamp (Pump ON)

This LED is ON when switch (4) above is in position '1' i.e. when dielectric pump is ON.

Push Button (AUTOPOS)

This is useful in position of the job. For actuation of this control, switch '20' has to be in position AUTO. On pressing this push button '20', the quill starts down slowly. As the electrode comes in the vicinity of workpiece (job), it maintains a constant gap at low voltage between the electrode and the workpiece with weak sparking. The AUTOPOS can be stopped by pressing push button '19' or by operation of preset depth switch on machine head.

Indicator Lamp (AUTOPOS)

This LED glows when AUTOPOS function starts by pressing push button '25' and becomes OFF when the function is stopped.

Piezo Ceramic Alarm (Buzzer)

This is an audio signal which indicates that the electrode has made contact with the workpiece. The function can be selected by a switch '28'. The buzzer sounds only when switch '10' is in MAN mode or when AUTOPOS is ON.

Toggle Switch (Buzzer Select)

This has two positions '0' and '1'. In position '1', the buzzer '27' is selected and in position '0' the buzzer '27' is selected.

Decade Counter (Hour Counter)

This counts the total machining time, i.e. the time counting is effective only during machining process. The counter counts continuously and hence the initial reading has to be recorded while counting machining time taken for any job. The least count is 0.01 hours.

2.5 Working Principle of EDM

When a difference of potential is applied between two conductors immersed in a dielectric fluid, the fluid will ionize if the potential difference reaches a high enough

value and a spark will occur. If the potential difference is maintained, then the spark will develop into an arc. If the potential difference decreases, the fluid will de-ionize and the discharge will cease.

In electric discharge machining process (Figure 2.5), the control of erosion of the metal is achieved by the rapidly recurring spark discharges produced between two electrodes, one tool and the other workpiece, and spark impinging against the surface of the workpiece which must be an electrically conductive body. A suitable gap known as "spark gap" is maintained between the tool and the workpiece by a servomotor which is actuated by the difference between a reference voltage and the gap breakdown voltage, which feeds the tool downwards towards the workpiece.

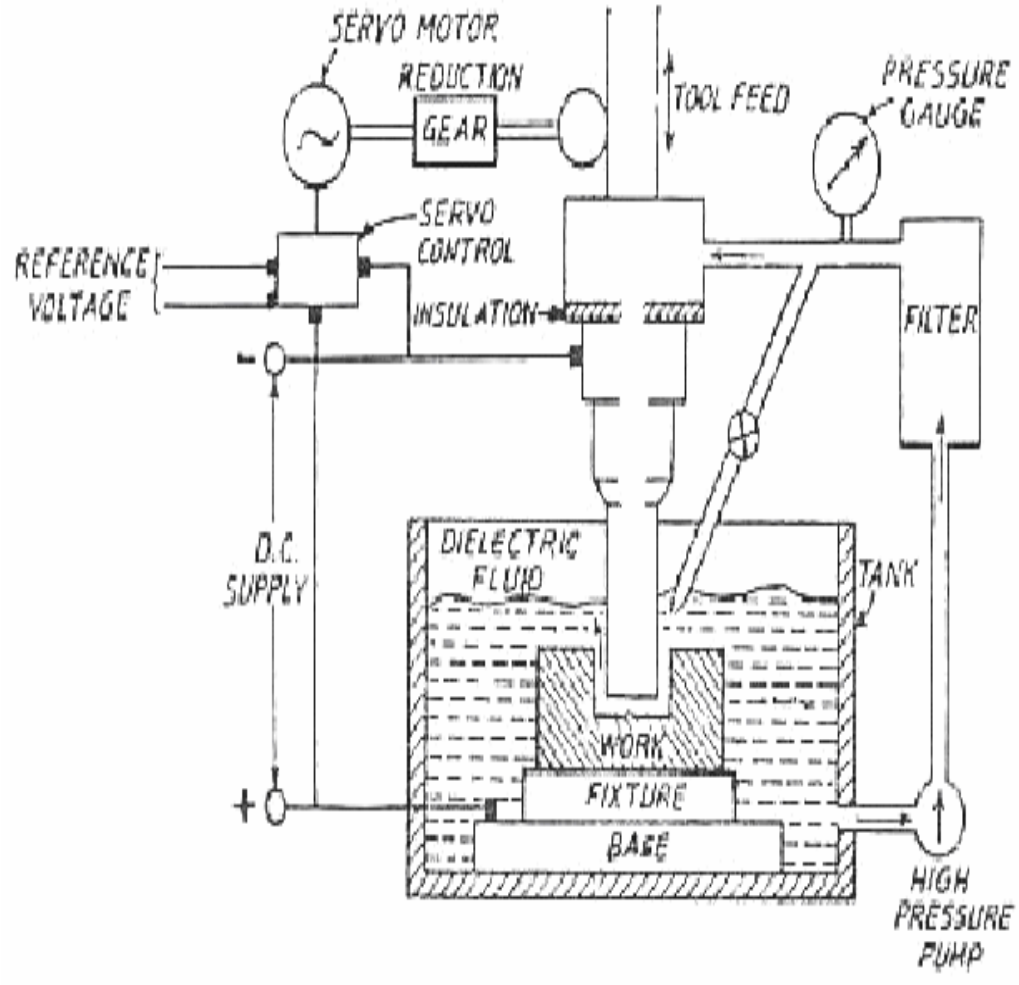

Figure 2.5: Schematic Diagram of EDM Process

The dielectric fluid fills up spark gap. The dielectric fluid may be typical hydrocarbon oil or de-ionized water which helps in cooling down the tool and the workpiece, cleans the inter-electrode gap, and concentrates the spark energy into small cross-sectional area under the electrode.

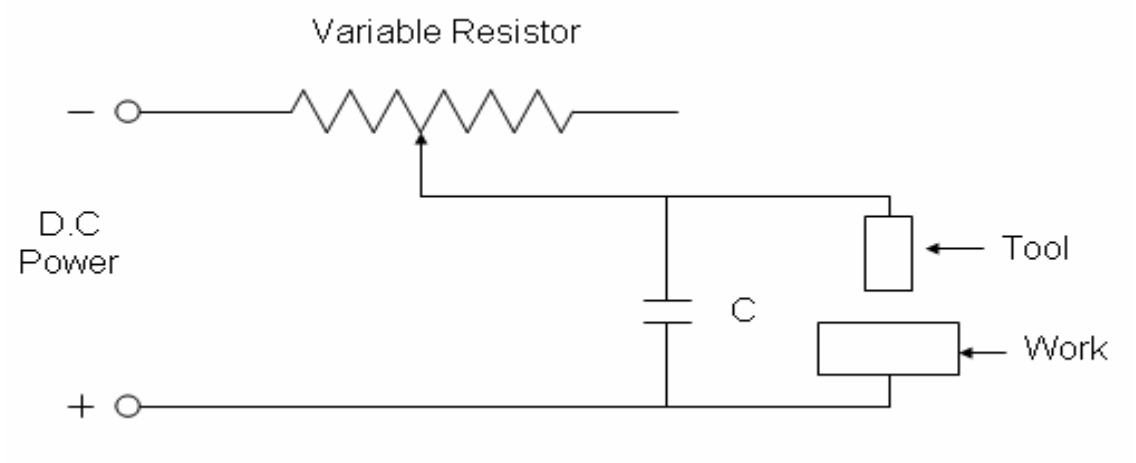

Figure 2.6: Working Principle of EDM

Each electric discharge or spark causes a focused stream of electrons to move with a very high velocity and acceleration from the cathode towards the anode, and ultimately creates compression shock waves on both the electrode surfaces, particularly at high spots on the workpiece surface, which are closest to the tool (Figure 2.6). The generation of compression shock waves, develops a local rise in temperature. The whole sequence of operation occurs within a few microseconds. However, the temperature of spot hit by the electrons is of the order of 10,000°C. This temperature is sufficient to melt a part of the metals. The force of electric and magnetic fields caused by a spark produce a tensile force and tear off particles of molten and softened metal from this spot in the workpiece. A part of the metal may vaporize and fill up the gap. The metal is thus removed in this way from the workpiece. The electric and magnetic fields on the heated metal cause a compressive force to act on the cathodic tool so that metal removal from the tool is at a slower rate than that from the workpiece. Hence, the workpiece is connected to the positive terminal and the tool to the negative terminal.

2.6 Process Parameters of EDM

Process Parameters which affect the performance of EDM are as given below:

Pulse on time

This is time period during which machining is performed. As the 'pulse on time' increases, machining will perform at faster a rate and craters will be broader and deeper thereby resulting in poor surface finish and high MRR.

Pulse off time

The 'pulse off' is the time during which re-ionization of the dielectric takes place. The more is the off time, the greater will be the machining time. The off time governs the stability of the process. An insufficient off time can lead to erratic cycling and retraction of the advancing servo thereby slowing down the operation cycle. Figure 2.7 shows the concept of pulse on time and pulse off time.

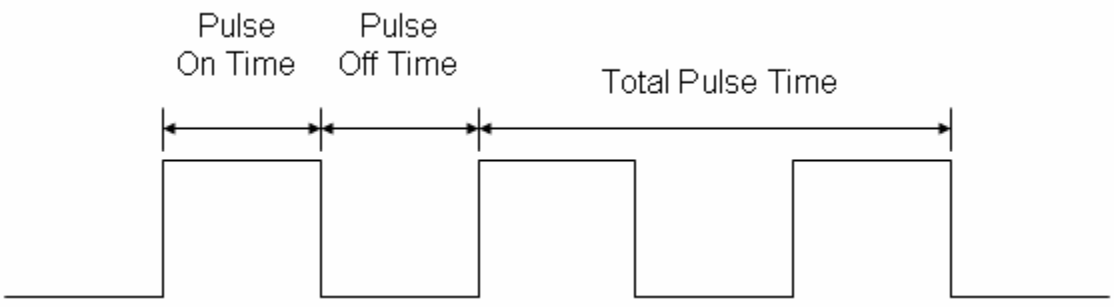

Figure 2.7: Concept of Pulse on Time and Pulse off Time

Peak current

The current is an average of the amperage in the spark gap measured over a complete cycle. This is read on the ammeter during the process. An increase in current results in increased MRR as well as increased value of SR. Figure 2.8 shows effect of current on surface

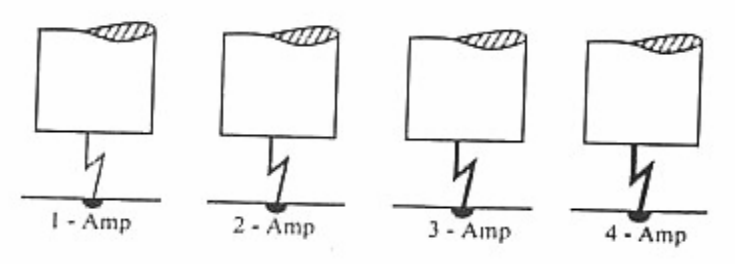

Figure 2.8: Effect of current during sparking on surface.

Gap voltage

The voltage applied is a DC power source of 40V to 400V. The preset voltage determines the width of spark gap between the leading edge of the electrode and the workpiece. High voltage setting increases the discharge gap and hence flushing and the machining.

Electrode gap size

The size of the gap is governed by the servo control system whose motion is controlled by gap width sensors. They control the motion of the ram head or the quill, which, in turn, governs the gap size. Typical values of the gap size range between 0.005 and 0.05 mm. The gap size governs the possibility of sparking and arcing. The gap size should be maintained enough to have proper flushing.

Duty factor

Duty factor is an important parameter in EDM process. This is given by the ratio of 'on time' to the 'total time'.

Electrode polarity

Polarity refers to the electric condition determining the direction of the current flow relative to the electrode. The polarity of the electrode can be either positive or negative depending on the application. Some electrodes give better results when the polarity is changed. The recommended polarity for different tool-jobs is given in Table 2.3 below:

Work material	Rougher	Finisher
Tool steel	+(*)	+ -
Stainless steel	+(*)	+ -
Aluminium	+ -	+ -
Titanium	-	-
Carbides	-	-
Copper	-	-

(*) = Negative polarity can be used when maximum speed is the only requirement.

Table 2.3: Recommended Polarities for different Tool-Job pairs.

Straight or normal polarity is that in which the tool is positive and the workpiece is negative, while in reverse polarity, tool is negative and the workpiece is positive. The concept of normal and reverse polarity is shown in Figure 2.9

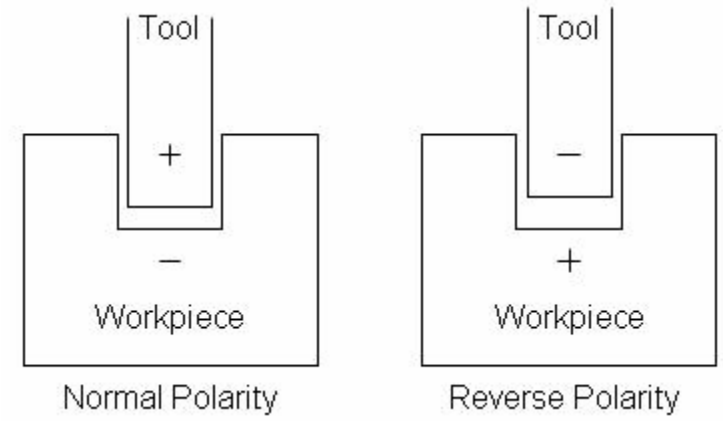

Figure 2.9: Concept of Normal Polarity and Reverse Polarity.

Frequency

This is a measure of the number of times the current is turned on and off. During roughing, the 'on time' is increased significantly for high removal rates and fewer cycles per second, hence a lower frequency setting as shown in Figure 2.10. Frequency is distinct from the duty cycle, as this is a measure of efficiency.

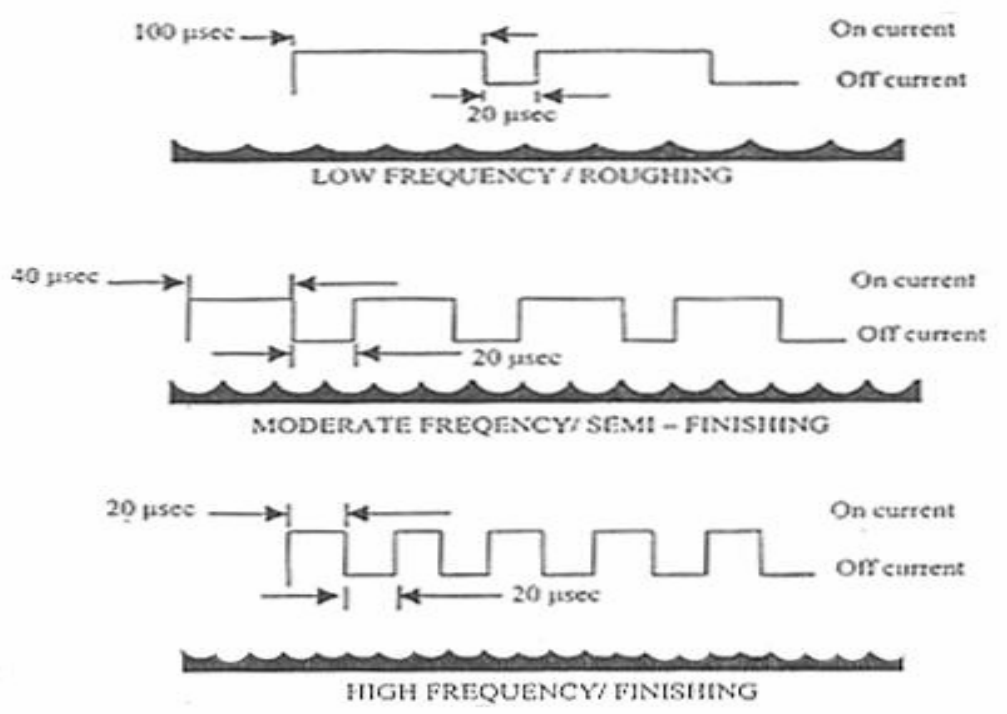

Figure 2.10: Effect of Frequency on Workpiece Surface.

The electrode (Tool)

The shape of the tool will be basically the same as that of the product desired. The material used for the tool influences the tool wear and the side clearance and hence, in turn, it has considerable influence on the rate of metal removal, finishing obtained, and the production rate. The electrode material generally used can be classified as metallic material (copper etc.), non-metallic materials (graphite), and combination of metallic and non-metallic materials (copper graphite). Copper, yellow brass, zinc, graphite and some other materials are used for tools. Low wearing tools include silver-tungsten, copper-tungsten, and metallized graphite. For commercial applications, copper is the best suited for fine machining, and cast iron is used for rough machining. One of the advantages of EDM is that a tool is made of a material softer than the workpiece material and which is a good conductor of electricity and can be used to machine a material of any hardness. The wear of the tool in the EDM process due to electron bombardment is inevitable. The tool wear rates determine the machining accuracy, tool movement and the consumption. The tool wear is a function of the rate of metal removal, material of the workpiece, current setting, machining area, gap between the tool and the work piece and the polarity of the

tool. It has been found that the higher the tool material melting point, the lesser the tool wears. Wear is best defined as:

$$\text{Wear Ratio} = \frac{\text{Volume of work material removed}}{\text{Volume of electrode consumed}}$$

This is often simplified to:

$$\text{Wear Ratio} = \frac{\text{Depth of cut}}{\text{Decrease in usable length of electrode}}$$

Dielectric fluids

The essential requirements of a dielectric fluid to be used in EDM process are that they should:

- Remain electrically non-conducting until the required breakdown voltage has been reached.
- Breakdown electrically in the shortest possible time once the breakdown voltage has been reached.
- Rapidly quench the spark or deionize the spark or spark gap after the discharges have occurred.
- Provide an effective cooling medium.
- Have good degree of fluidity.

Material removal rate (MRR)

The material removal rate is generally described as the volume of metal removed per unit time. The material being cut will affect the MRR which varies inversely as the melting point of the metal.

Chapter-3
Review of Literature

Electric discharge machining has been widely used for manufacturing various components such as moulds/dies and aero-engine parts. However, it has been observed that a brittle cracked white layer on the surface is formed in conventional sinking EDM. In order to realize mirror like finished surface of large area with less crack, surface modification techniques need to be investigated. Relevant literature pertaining to surface modification has, therefore, been reviewed as given below:

Mohri *et al.* (1993) conducted studies on a new method of surface modification by electrical discharge machining using composite structured electrode. Surface modifications on workpiece of carbon steel and aluminium were carried out in hydrocarbon oil using composite electrodes. Composite electrode consisted of green compact products or sintered electrode products. It was revealed that there existed the electrode material in the work surface layer, and the characteristics of the surface of the raw material remarkably changed. These surfaces had less cracks and higher corrosion resistance.

Ming and He (1995) studied the effects of additives in kerosene used as the dielectric fluid for EDM. It was observed that the additives could increase the MRR and decrease the TWR and improve the surface quality of the work quite clearly, especially in mid-finish machining and finish machining. Some additives used in the tests were introduced and their mechanism was discussed.

Zhixin *et al.* (1995) developed a mechanical pulse electric discharge machining (MPEDM) technique to produce holes in the conductive hard and brittle materials, and the mechanism of the MPEDM was described. The sparks of the electric discharge in the MPEDM were caused by the ultrasonic vibration of the tool which was used in place of the conventional special pulse generator. Ultrasonic vibration of the tool also acted as gap-flushing method. Tap water was used as the working fluid in the MPEDM technique. It was confirmed that the MPEDM was effective to attain a higher material removal rate (MRR) for a conductive difficult-to-machine materials.

Ker *et al.* (1998) proposed a new output electro-static discharge (ESD) protection in order to provide area-efficient output ESD protection for the scaled down CMOS VLSI. In the new output ESD protection circuit, there were two novel devices, the PTLSCR (PMO-trigger lateral SCR) and the NTLSCR (NMOS-trigger lateral SCR). The PTLSCR and NTLSCR were guaranteed to be turned on first before the output PMOS or NMOS were broken down by the ESD voltage. Ker and coworkers further observed that PTLSCR and NTLSCR could sustain over 4000V (700V) of the human body model (machine model) ESD stress within a very small layout area in a 0.6 μm CMOS technology with LDD and polycide processes. The noise margin of the proposed output ESD protection was greater than 8V (lower than -3.3V) to avoid the undesired triggering on the NTLSCR (PTLSCR) due to the overshooting (undershooting) voltage pulse on the output pad when the IC was under normal operating conditions with 5V VDD and 0V power supplies.

Chen and Mahdavian (1999) conducted experiments with different values of discharge current, pulse duration time and interval time in EDM to investigate their effects on the material removal rate, surface quality and dimensional accuracy of the tool and product. Optimum pulse duration and pulse interval values in EDM that either produced the highest erosion rate or fine surface finishes were shown to have significant importance to the machinery process.

Hsue *et al.* (1999) studied fundamental geometry properties of wire electrical discharge machining (WEDM) process in corner cutting. They introduced the concept of discharge-angle and derived its mathematical expression by analytical geometry. A model to estimate the metal removal rate (MRR) in geometrical cutting was developed by considering wire deflection with transformed exponential trajectory of wire centre. Both of the discharge angle and MRR dropped drastically to a minimum value depending on the corner angle being cut as the guides arrived at the corner apex and recovered to the same level of straight-path cutting sluggishly. In addition, the variation of the machining load caused by the change of MRR, which was taken as unknown disturbance in the past, could be predicted and used for control purpose.

Park *et al.* (1999) hot-pressed titanium diboride (TiB_2) at a temperature of 1800°C, and added silicon nitride (Si_3N_4) as sintering aid. When a small amount (2.5 wt %) of Si_3N_4 was added, the Si_3N_4 reacted with titania (TiO_2) that was present on the surface of the TiB_2 powder to form titanium nitride (TiN), boron nitride (BN) and amorphous silica (SiO_2). The elimination of TiO_2 suppressed the grain growth effectively which led to an improvement in the densification of TiB_2. The formation of SiO_2 also was deemed beneficial for densification. The mechanical properties especially the flexural strength were enhanced remarkably through these improvements in the sinterability and microstructure.

Hu and Dean (2000) investigated the relation between friction behaviour and surface topography using various lubricants and initial workpiece surface condition in ring upsetting and rod extrusion processes. It was found that smoother ones could retain more lubricant and decrease friction resistance for random surfaces. Turned surfaces were found to be effective in reducing friction, but the final surface finish of the workpiece was not as good as that from random surfaces.

Kunieda and Ojima (2000) described the improvement of the machinery rate of EDM for silicon single crystals by reducing the contact resistance between the silicon single crystal and metal electric feeder. Efforts were made to decrease the resistance of the rectifying contact between a p-type silicon wafer and the metal feeder for achieving ohmic contact by plating the contact surface of the silicon wafer with aluminium by vacuum evaporation followed by the diffusion process. Gold-antimony alloy was used in place of aluminium in order to accomplish an ohmic contact between n-type silicon and metal. The influence of polarity on the machinery rate was also discussed from the view point of the rectifying nature of the interface between the arc plasma and silicon single crystal.

Stampfi *et al.* (2000) used micromachined silicon as a mould for electroplating copper and for hot-processing silver tungsten. After removing the silicon, the copper or silver- tungsten was used as an electrode for electro-discharge machining. Using these process steps, nearly any conductive material could be shaped in particular magnetic materials like amorphous metal which were difficult or impossible to machine otherwise.

The researchers described the fabrication of the electrodes as well as the influence of the electrode material on the achieved quality of the final part.

Furutani *et al.* (2001) attempted to make thick titanium carbide (TiC) or WC layer and investigated a surface modification method by EDM with a green compact electrode. Titanium alloy powder or tungsten powder was supplied from the green compact electrode and it adhered on a workpiece by the heat caused by discharge. They proposed a surface modification method by EDM with powder suspended in working fluid in order to avoid the production process of the green compact electrode. According to the investigators, the use of a thin electrode and a rotating disk electrode were expected to keep powder concentration high in the gap between a workpiece and an electrode and to accrete powder material on the workpiece. Titanium powder was suspended in working oil like kerosene. TiC layer developed a thickness of 150 μm with a hardness of 1600 HV on carbon steel with an electrode of 1 mm in diameter. When a disk placed near a plate rotates in viscous fluid, the disk dragged the fluid into the gap between the disk and the plate. Hence, the powder concentration in the gap between a workpiece and a rotational disk electrode could be kept high. A wider area of the accretion could be obtained by using the rotational electrode with a gear shape.

Kawaoka *et al.* (2001) suggested a new approach to provide an electrical conductivity to insulator structural ceramics. In this concept, sintering additives formed conductive network after sintering and resulted in a great reduction of amount of conductive phase addition compared with particle dispersion method generally used. Na^+ ionic-conductive silicon nitride and Na^+ ionic-conductive magnesia ceramics were successfully fabricated by this method.

Ghoreishi and Atkinson (2002) compared the effects of high and low frequency forced axial vibration of the electrode, rotation of the electrode and combinations of these methods in respect of material removal rate (MRR), tool wear rate and surface roughness in die sinking electro-discharge machining(EDM) with a flat electrode (planning mode). It was found that the combination of high frequency vibration and rotation of the electrode was effective in attaining a high MRR at a specified surface roughness (Ra).

Sanchez *et al.* (2002) assessed the validity of different multi-stage planetary EDM strategies from the point of view of machining time and surface finish. However, the

optimum choice under these criteria did not assure that dimensional accuracy requirements were met. Thus, the different error sources were analyzed paying most attention to thermally induced errors which were numerically simulated from experimental data collected during the process.

Yan *et al.* (2002) investigated feasibility of modifying the surface of Al-Zn-Mg alloy by a combined process of electric discharge machinery (EDM) with ball burnish machining (BBM). They reported that the combined process could effectively improve the surface roughness to obtain a fine finishing and flat surface. The micropores and cracks caused from EDM were eliminated during the process as well. Further more, such a process could reinforce and increase the corrosion resistance of the machined surface after machining.

Furutani and Shimizu (2003) investigated the deposition process of lubricant surface by EDM with Molybdenum disulfide (MoS_2) powder suspended in working oil. They also studied the influence of some machining conditions through the friction test. It was found that MoS_2 could be deposited on metals which had melting point lower than MoS_2. The expansion of the gap length caused the improvement of the roughness.

Puri and Bhattacharya (2003) considered all the machine control parameters simultaneously for the machining operation which comprised a rough cut followed by a trim cut. They carried out the investigation based on the Taguchi method involving thirteen control factors with three levels for an orthogonal array L_{27} (13^{13}). The main influencing factors were determined for given machining criteria such as average cutting speed, surface finish characteristics and geometrical inaccuracy caused due to wire lag. The optimum parametric settings for different machining situations had also been found out.

Pecas and Henriques (2003) studied the performance improvement of conventional EDM when used with a powder mixed dielectric. They used silicon powder and assessed the improvement through quality surface indicators and process time measurements over a set of different processing areas. They observed that silicon powder showed a positive influence in the reduction of the operating time required to achieve a specific surface quality, and in the decrease of the surface roughness, allowing the generation of mirror-like surfaces.

Simao *et al.* (2003) reviewed the published work on the deliberate alloying of various workpiece materials using EDM. Details have been given of operations involving powder metallurgy (PM) tool electrodes and the use of powders suspended in the dielectric fluid, typically aluminium, nickel, titanium etc. Results have been presented on the surface alloying of AISIH13 hot work tool steel during a die sink operation using partially sintered WC / Co electrodes operating in a hydrocarbon oil dielectric. An LS fractional factorial Taguchi experiment was used to identify the effect of key operating factors on output measures viz., electrode wear, workpiece surface hardness, etc. With respect to microhardness, the percentage contribution ratios (PCR) for peak current, electrode polarity and pulse on time were approximately 24, 20 and 19%, respectively. Typically, changes in surface metallurgy were measured upto a depth of about 30 μm (with a higher than normal voltage of about 270V) and an increase in the surface hardness of the recast layer varying from 620 HK 0.025 to 1350 HK 0.025 approximately.

Wang and Ravani (2003) developed a computational method for numerical control (NC) of traveling wire electrical discharge machining (EDM) operation from geometric representation of a desired cut profile in terms of its contours. Normalized arc length parameterization of the contour curves was used to represent the cut profile and a subdivision algorithm was developed together with kinematic analysis to generate the required motions of the machine tool axis. In generating the tool motions for cutting sections with high curvatures such as corners with small radii, a geometric path lifting method was presented that increased the machining gap and prevented gauging or wire breakage.

Chang and Chiu (2004) applied robust control to compensate for electrode wear in an electric discharge scanning (ED-scanning) process. This control compensated for the wear without reference to the wear ratio of electrodes. An auxilary gap-control loop in the vertical direction could compensate for the wear of the electrode, according to the discharge voltage when the electrode was driven along the two horizontal axis. A proportional controller for a gap-control system with minimum robustness was designed and robustly analyzed to override the non-linear and time varying feedback. The controller could maintain the location of the discharge on the vertical axis and fix the depth of the removal to that of a particular layer. The practical scanning process revealed

that the dimension of the hole could be guaranteed only if the data concerning the depth of the removal under specific discharge conditions and electrode diameters were applied.

Han and Kunieda (2004) described the development of parallel spark EDM method. Compared with conventional EDM in which only a singular discharge could be generated for each pulse, multiple discharges could be generated for each pulse in parallel spark EDM. Machining process was not only more stable but the machining speed and surface roughness could also be improved with parallel spark EDM.

Han *et al*. (2004) developed a new transistor type isopulse generator using a current sensor with high frequency response. The pulse duration could be reduced to about 30 nano-seconds, which was equivalent to the pulse duration used in finishing by the conventional RC pulse generator for micro-EDM. In order to achieve stable machining and improve machining characteristics, a new servo feed control system for micro-EDM using average ignition delay time to monitor the gap system was developed. By integrating the transistor type isopulse generator with this new servo feed control system, it was possible to obtain a removal rate of about 24 times higher than that of the conventional RC pulse generator with a constant feed rate in both semi-finishing and finishing. The effectiveness of the servo feed control proved higher in finishing than in semi-finishing, whereas the transistor type isopulse generator was more effective in semi-finishing than in finishing.

Ho *et al.* (2004) reviewed a large array of research work on wire electrical discharge machinery (WEDM) involving the optimization of the process parameters surveying the influence of the various factors affecting the machinery performance and productivity. In the past, there has been a risk of wire breakage and bending which undermined the full potential of the process (WEDM) drastically reducing the efficiency and accuracy of the WEDM operation.

Klocke *et al.* (2004) examined the effects on the recent layer by using micro Joule-range discharge energies in combination with powder suspended working fluids. Effects of a capacitor connected parallel to the gap were investigated in relation to the recent layer formation. In addition, transverse section pictures showed the morphology and the depth of the thermal influenced zone. It was aimed at investigating the influence of the powder particles in micro-sinking –EDM and especially in the gap on the thermal spread

in the dielectric and on the influenced zone. Furthermore, a complete qualitative and quantitative analysis of an EDX spectrum had been performed in order to examine the changes of the recent layer composition by using powder suspended dielectric at the workpiece surface.

Moro *et al.* (2004) studied the application technology of electrical discharge coating (EDC) to improve cutting tool life by electrical discharge machining (EDM) instead of physical vapour deposition (PVD) or chemical vapour deposition (CVD). EDC tools were found to be limited to the application of low cutting speed conditions such as a drill. It was further observed that the worn amount of EDC coated drills was caused by high friction coefficient and this high friction coefficient was led by surface roughness. The application of grinding machine was available under the high precision machining in order to reduce the surface roughness.

Pham *et al.* (2004) presented some recent developments in micro-EDM in its various forms (wire, drilling, milling and die-sinking) and discussed the main research issues. The investigations planned the EDM process and the electrode wear problem. Special attention was paid to factors and procedures influencing the accuracy achievable including positioning approaches during EDM and electrode grinding.

Rehbein *et al.* (2004) determined the ignition and breakdown behaviour in spark erosion process by a large number of different effects. The investigators revealed specific effects of some selected groups of additives which were added to the dielectric working fluid. Efforts were made to find additives which led to modified discharge channels. The first investigation referred to those groups of additives which could be found in commonly available spark erosion fluids depending upon the production process. The example indicated the different breakdown courses of alicylic aromatic hydrocarbons.

Chang (2005) designed a robust proportional plus derivative (PD) controller of the gap between an electrode and a workpiece to tolerate the bounded gain variation related to the generation of powder in the gap and the non-linearity of the feedback signal. The robustness (H∞) showed that the robust PD controller could tolerate the non-linear and time-varying feedback signals and performance of H_2 under a constraint on H∞ robustness. The proposed PD controller exhibited optimal tracking performance. The gain parameters of the PD controller that maximized fitness, as specified by the inverse of the

integral of the squared error, given a step input to the system, could be determined quickly and accurately using genetic algorithms (GAs). The control performance and the rate of erosion of die-sinking EDMs were confirmed to follow from the proposed design procedure.

Wu *et al.* (2005) investigated the effect of surfactant and Al powders added in the dielectric on the surface status of the workpiece after EDM. It was found that the best distribution effect was produced when the concentrations of the Al powder and surfactant in the dielectric were 0.1 and 0.25 g/l, respectively. An optimal surface roughness (Ra) value of 0.172 μm was achieved under positive polarity, discharge current 0.3 A, pulse duration time 1.5 μs, open circuit potential 140V, gap voltage 90 V and surfactant concentration 0.25 g/l. The surface roughness status of the workpiece was improved upto 60% as compared to that EDMed under pure dielectric with high surface roughness Ra of 0.434 μm.

Chang and Hong (2005) compared a buffered digital differential analyzer (BDDA) algorithm with the reference-word interpolation and real-time polynominal interpolation used in a milling EDM to confirm improvements of erosion speed. The proposed algorithm in a computerized numerical controller (CNC) performed milling electric discharge machining of a curve constructed from a sequence of segments using a traditional computer aided manufacturing (CAM) system. The proposed algorithm interpolated more than one segment in a sampling interval and supported the effective machining of a parametric curve when the electrode crossed the connection between the short segments. The accuracy of both the speed and the trajectory of motion could be ensured without the time function of the parameter specified by two terms of a Taylor expansion, such as in a real-time parametric curve interpolator.

Miller *et al.* (2005) explored the use of wire EDM for manufacturing of complaint mechanisms and studied the wire EDM of cross-section with minimum thickness and complaint mechanisms. The researchers investigated the effects of EDM process parameters, particularly the spark cycle time and spark on-time on thin cross-section cutting of Nd-Fe-B magnetic material, carbon bipolar plate, and titanium. An envelope of feasible wire EDM process parameters was generated for the commercially pure titanium. The investigators demonstrated the application of such envelope to select suitable EDM

process parameters for micro feature generation. Scanning electron microscopy (SEM) analysis of EDM surface, sub-surface and debris have been presented. SEM observations led to a hypothesis based on the thermal and electrostatic stress induced fracture to explain the limiting factor for wire EDM cutting of thin sections.

Ekmekci *et al.* (2005) used layer removal method to measure the residual stress profile as a function of depth beneath the surface caused by die sinking type electric discharge machining. They also studied cracking and its consequences on residual stresses on samples machined at long pulse durations. They developed a modified empirical equation for scaling residual stresses in machined surfaces with respect to operating conditions. In this model, a unit amplitude shape function representing change in curvature with respect to removal depth was proposed. The proposed form was found to be a special form of a Gauss Distribution. It is the sum of two Gaussian peaks, with the same amplitude and pulse width but opposite centre location. The form can be represented by three constant coefficients. These coefficients depend on the released energy by a power function.

Janousek *et al.* (2005) evaluated deep surface-breaking cracks in the front face of thick structures and suggested the usefulness of eddy current testing while keeping the advantages of higher frequency inspection. The studies helped in suppressing the eddy currents on the surface of a test piece thereby realizing the deeper penetration of eddy currents. They have designed a mutual induction eddy current testing probe which consisted of four coaxial rectangular tangential exciter coils and a pancake pick-up coil. The exciters are driven by AC currents with different phases and amplitudes which contrive to emulate the desired behaviour. When the new probe was used for inspections under a frequency of 10 KHz, there was a 20% difference between signals due to an electro-discharge machined (EDM) notch of 15 mm depth and those due to one of 20 mm depth. On the other hand, a conventional probe driven with the same frequency gave only 1% difference between the signals of the two EDM notches.

Ramaswamy *et al.* (2005) investigated the effect of the EDM main process parameters on the average thickness of the white layer, and developed related empirical correlation equations with the 3D amplitude and spatial surface texture parameters, and provided possible physical explanation for the validity of these mathematical

relationships. They obtained a better correlation between the average thickness of the white layer (AWLT) and the spatial parameter (Sds) as compared to other 3D surface texture parameters. It might be attributed to the similar effect of the current and pulse on-time on both AWLT and Sds. The possible effect of surface tension between the solid and liquid phases on the thickness of the white layer during erosion was also discussed.

Marafona and Chousal (2005) developed a model to represent the electrical discharge in EDM based on the Joule heating effect in the dielectric using Finite Element Analysis (FEA). The main aim of developing this model was to predict the removed material from tool and workpiece as well as the maximum temperature reached in the discharge channel. A thermal-electrical model was developed for sparks generated by electrical discharge in a liquid medium. In this model, the radii value of the conductor is a function of the current intensity and pulse duration. The thermal-physical values used in the model were the average both the ambient and melting values. Copper and iron were the materials used for anode and cathode respectively. The Finite Element Analysis (FEA) results were compared with the experimental values of the table of AGIE SIT. In order to show the universality of the model, results were obtained for all current intensity values of the table. The Tool Wear Ratio (TWR) and Material Removal Rate (MRR) as well as surface roughness results agreed reasonably well with the researcher's values.

Lin *et al* (2005) examined the characteristics of micro-EDM applied to high nickel alloy and evaluated the effectiveness of HFDG by observing the surface roughness of the micro-hole inner-wall. As judged from SEM photographs and surface roughness measurements, they reported that HFDG method could reduce surface roughness from 2.12 to 0.85 μM Rmax with micro-cracks eliminated. They also demonstrated that micro-holes fabricated by micro-EDM at peak current 500 mA followed by HFDG at 40V could achieve precise shape and good surface quality after 6-8 min of lapping.

Chapter-4

Materials and Methods

Study on the research problem entitled "Experimental investigation on surface modification with powder mixed dielectric discharge machining" were conducted in the Mechanical Engineering Department and R and D centre, Thapar Institute of Engineering and Technology, Patiala during the year 2006.

4.1 Experimental Details

The dielectric system of EDM needed about 50 litres of dielectric fluid (Kerosene) for the circulation of dielectric under existing conditions. A huge amount of dielectric fluid would be consumed for conducting a large number of experiments that requires different levels of concentration of powders. So, it was not possible to circulate the powder mixed dielectric fluid in the existing set-up because the filter might get choked. Therefore, a new experimental set-up was designed which contained the following components:

1. Mild steel tank
2. Workpiece fixture assembly
3. Stirrer assembly

This system needed only 7 litres of dielectric fluid for experiment. It consisted of a mild steel tank, which was inserted in the dielectric tank of EDM. It was filled up with powder suspended dielectric. A stirrer was also employed in order to prevent precipitation of Al_2O_3 and SiC powder. A pure copper electrode was used as a tool electrode.

4.2 Equipments and Materials

4.2.1 Details of Equipments

Tank

It was made up of mild steel and was placed in the dielectric sump of EDM. The capacity of the tank is 7 liters. These dimensions were taken so that the tank would be filled with sufficient dielectric fluid, which would be circulated for cooling the tool electrode and workpiece during the pulse off time. Figure 4.1 shows the different views of the tank.

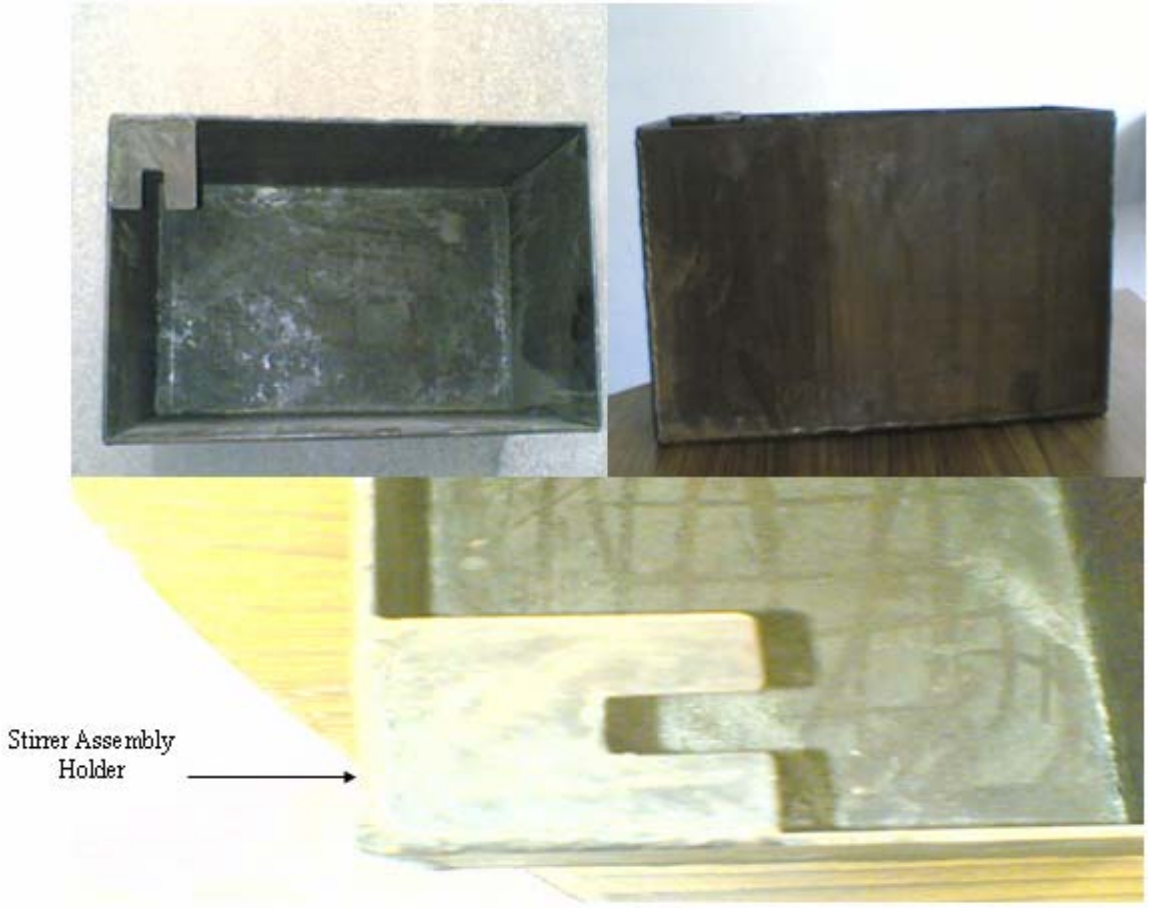

Figure 4.1: Showing Different Views of Tank

Workpiece Fixture Assembly

It was used to hold, locate and fix the workpiece firmly. Figure 4.2 shows the different views of workpiece fixture assembly.

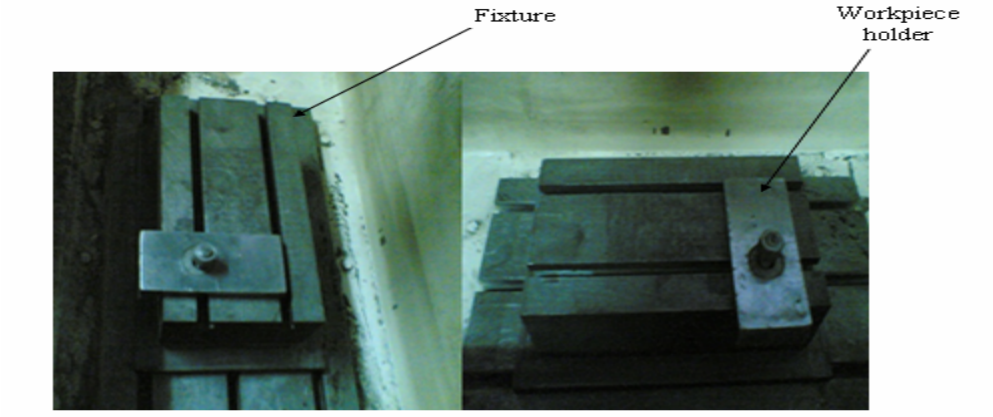

Figure 4.2: Workpiece Fixture Assembly

Stirrer Assembly

A stirrer was employed in the container where machining was performed. It was used to prevent deposition of Al_2O_3 and SiC powders at the bottom of the container, and mixing of powders properly took place. It is shown in Figure 4.3.

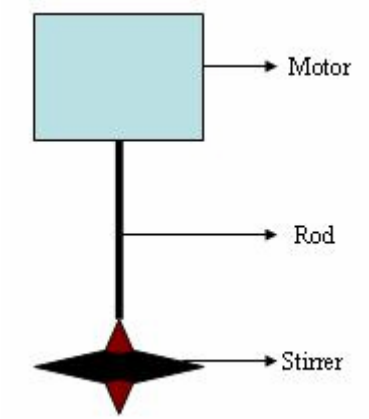

Figure 4.3: Stirrer Assembly

4.2.2 Details of the Consumables

Workpiece Material

The workpiece material taken for this study was EN 24 steel. Twelve plates were used for marching work; two plates are shown in Figure 4.4. Its composition is presented in Table 4.1 as given below:

C	Mn	P	S	Si	Cr	Ni	Mo
0.44 %	0.45 %	0.025%	0.025%	0.15 %	1.40%	1.50%	0.35%

Table 4.1: Chemical Composition of EN 24 Steel.

Figure 4.4: Workpiece EN 24 Steel

Tool Material

The tool material selected for this investigation was pure copper. The electrode (Figure 4.5 and 4.6) is in the form of a circular rod of diameter 14.9 mm at the point of spark. The properties of copper electrode are given below in Table 4.2.

Density	Electrical Receptivity	Purity	Melting Point
8.9 kg/m^3	0.0167 Ωmm^2/m	99.9%	1083 °C

Table 4.2: Properties of Copper Electrode

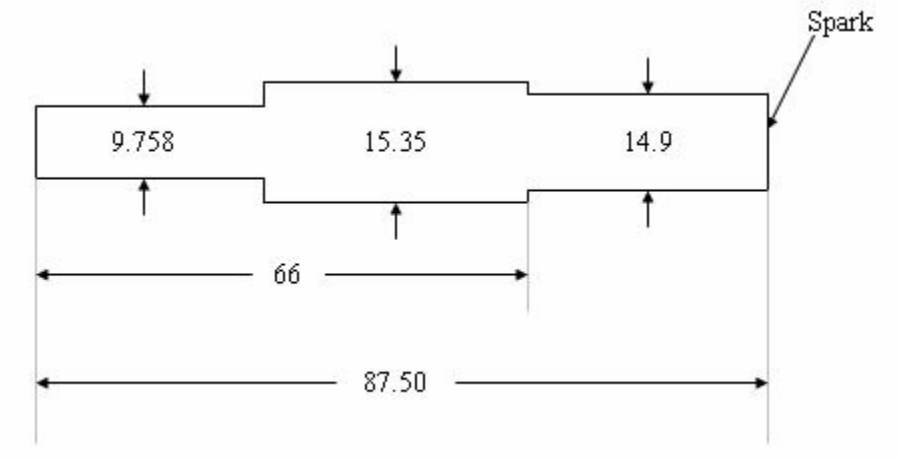

Figure 4.5: Showing Dimensions (mm) of Copper Electrode.

Figure 4.6: Showing Different Views of Copper Electrode.

Dielectric Fluid

The dielectric fluid used for experimentation was commercial grade kerosene. Table 4.3 shows the properties of kerosene oil.

Surface Tension (N/m)	Density (kg/m^3)	Dynamic Viscosity (Pas)
0.028	820	2400

Table 4.3: Properties of Commercial Grade Kerosene.

Powders Used for Experimentation

Two powders were used as given below:

i. Al_2O_3 active neutral, and

ii. SiC.

Specifications and colours of both powders are given as under:

1. Al_2O_3 active neutral.

a) Specifications

Property	Specifications	
pH	7.0 ± 0.5	
Mesh size	100-300	
Limits of impurities	Chlorine (Cl)	0.1 %
	Sulphate (SO_4)	0.1 %
	Water solubles	0.5 %

Table 4.4: Specifications of Al_2O_3 active neutral.

b) Colour: As evident from the Figure 4.7, the colour of Al_2O_3 active neutral is white.

Figure 4.7: Showing colour of Al_2O_3 active neutral

2. SiC.

a) Specifications

Property	Specification
Mesh size	400

Table 4.5: Specifications of SiC.

b) Colour: As evident from the Figure 4.8, the colour of SiC is green.

Figure 4.8: Shows colour of SiC

4.3 Methodology

4.3.1 Specimen Preparation

Material	:	EN-24 Steel.
Hardness	:	49-50 HRc.

Cleaning

All the undesirable particles viz. foreign material, oil, scale, rust, grease, etc. is removed with the help of grinding process. Thinner was used after accomplishing grinding process for proper cleaning of surface.

Machining

Machining was performed on a locally designed tool craft EDM machine located in the Machine Tool Lab at Thapar Institute of Engineering and Technology, Patiala. Pure copper electrodes were used to machine EN-24 steel. The workpiece was used to machine surface in different dielectric fluids i.e. kerosene, Al_2O_3 mixed kerosene and SiC mixed kerosene.

4.3.2 Process Parameters (Input Variables)

The process parameters that were chosen for experimentation are given as under:

1. Concentration of added powder (g/l)
2. Peak current
3. Pulse on time (μs)
4. Pulse off time (μs)
5. Electrode lift time (sec)
6. Gap (mm)
7. Straight polarity
8. Reverse polarity

The levels of each input parameter were decided by studying the literature in detailed.

Values of Different Fixed Input Variables

Supply Voltage	:	110 volts.
Machining time for 1 cut	:	20 minutes.
No. of cuts (Machining)	:	84
Tool material	:	Copper
Tool size	:	Ø 14.9 mm for both Al_2O_3 and SiC.
Workpiece material	:	EN 24

Parameters	Levels					
	1	2	3	4	5	6
Concentration of added powder (g/l)	0/2/8/16	0/2/8/16	0/2/8/16	0/2/8/16	0/2/8/16	0/2/8/16
Peak current (Amp)	4	4	5	5	6	6
Pulse on time (μs)	4	5	4	5	4	5
Pulse off time (μs)	6	6	6	6	6	6
Electrode lift time (sec.)	1	1	1	1	1	1
Gap (mm)	0.2	0.2	0.2	0.2	0.2	0.2

Table 4.6: Process parameters with straight and reverse polarity with/without using powders of different concentrations.

Output Parameters

The following output parameters were studied during the course of this experimentation:

1. Microstructure.
2. Material Removal Rate (MRR) of both tool and workpiece.
3. Surface hardness.
4. Surface roughness.

4.4 Analysis of Machined Surface

Experiments were carried out on EDM model no. T – 3822M. The parameters chosen for study were microstructure, material Removal Rate (MRR) of tool and workpiece, surface hardness and surface roughness at different PMEDM parameter levels as mentioned in table. A total number of 84 experiments were performed by with/without addition of Al_2O_3 active neutral and SiC powders of different concentrations. Experiments were done on both straight and reverse polarity.

Following equipments were used to obtain the results for:

Material Removal Rate

The material removal rate (MRR) of both tool and the workpiece was calculated by measuring the weight of both tool and the workpiece after each machining period. For this, Weighing machine was used which is as shown in Figure 4.9.

Figure 4.9: Weighing machine

The Basic specifications of Weighting Machine are given as under:

1. Type : Resistance.
2. Measurement ranges : 500 g (max.)

Surface Roughness

The surface roughness of each hole of workpiece was measured four times and then the averages of the four readings were considered to decrease the error. The SR of straight polarity workpieces were measured on "Perthometer M4Pi" (Figure 4.10) in the Metrology Department. The basic specifications of surface roughness tester "Perthometer M4Pi" are given as follows:

Figure 4.10: Perthometer M4Pi.

1. Principle of measurement : Stylus method
2. Measurement ranges : 100 - 150 µm
3. Cut-off wavelengths : 0.08 – **0.25** – 0.8 – 2.5 mm
4. Tracing lengths : 1.5 – **4.8** – 15 mm
5. Number of sampling lengths : 1……5 selectable
6. Parameters : **R_a**, R_q, R_z, R_{max}, R_p, **R_t**, M_r (material ratio)
7. Tolerance monitoring : Max./min. for all parameters selected.
8. Measuring unit : µm, µin selectable
9. Dimensions (W x D x H) : 175 x 85 x 70 mm
10. Weight : Approx. 600g

The surface roughnesses of reverse polarity machined workpieces were measured on "Surf Test" in the Metrology Department.

The basic specifications of Surf Test are given as under:

1. Detector
    - Detecting system : Moving Magnet System.
    - Materials of Stylus : Diamond
    - Tip Radius : 10 ± 2.5 mm
    - Tip Angle : 90° + 10

- Measuring Force : 14.7 N
- Skid Radius : 15 mm
- Measurable Depth : 1.08

2. Power Drive
    - Driving Speed : 2 mm/sec or 6 mm/sec.
    - Driving Range : 2-50 mm
3. Amplifier/Meter
    - Indicating System
    - R_a - Center Line Average (Continuous Indicating System).
    - R_t - Peak to valley (Peak Retaining System).

Surface Hardness

The surface hardness of each hole was measured by Rockwell Hardness Tester (Figure 4.11) on C-scale by using diamond cone 60° indentor at a load of 150 kg.

Figure 4.11: Rockwell Hardness Tester.

Microstructure Testing

Scanning Electron Microscope (SEM) (Figure 4.12) was used to analyze the microstructure of workpiece. About 14 nos. of machined surfaces were examined (2 nos.

simple process straight and reverse polarity, 6 nos. Al_2O_3 active neutral straight and reverse polarity, and 6 nos. SiC straight and reverse polarity).

Figure 4.12: Scanning Electron Microscope (SEM).

The specifications of SEM are given as under:

1. Model No. : JSM - 840A
2. Magnification : $10X^{-3}$ x 10^5X
3. Company : Jeol, JAPAN

Chapter-5

Results and Discussion

Experiments were carried out on a powder mixed EDM (machine model no. T-38822 M) with straight as well as reverse polarity. After machining of the specimens by using different experimental conditions as mentioned in the previous chapter, the following results were obtained:

5.2 Roughness Analysis of Machined Surfaces

Straight Polarity Machined Surfaces

Surface roughness of each hole of workpiece was measured four times and then the average of the four was considered to decrease the error.

Figure 5.1: Straight polarity machined surfaces with/without addition of powders.

Reverse Polarity Machined Surfaces

Figure 5.2: Reverse polarity machined surfaces with/without addition of powders.

All the above workpieces as shown in Figures 5.1 and 5.2 were examined with the help of "perthometer" and "surf test" instruments respectively.

Surface Roughness (Ra) Analysis (Cut off value = .25 and tracing = 1.5 mm)							
Parame-ters	Straight Polarity Process						
	Simple	Al_2O_3 (Con.=2 g/l)	Al_2O_3 (Con.=8g/l)	Al_2O_3 (Con.=16 g/l)	SiC (Con.=2 g/l)	SiC (Con.=8 g/l)	SiC (Con.=16 g/l)
Pc=4 Pon=4 Poff=6	4.23	4.90	4.02	3.64	4.00	4.01	3.47
Pc=4 Pon=5 Poff=6	4.96	4.08	3.78	4.36	4.11	4.08	4.33
Pc=5 Pon=4 Poff=6	4.70	4.09	4.93	3.55	4.08	4.24	3.44
Pc=5 Pon=5 Poff=6	4.50	4.49	4.55	4.37	4.37	4.25	4.31
Pc=6 Pon=4 Poff=6	4.70	5.05	4.62	4.29	4.14	4.33	4.21
Pc=6 Pon=5 Poff=6	5.00	4.60	4.66	4.55	4.38	4.54	4.50

Table 5.1: Showing different values of surface roughness for various parameters.

Where Pc = Peak current in amp, Pon = Pulse on time, and Poff = Pulse off time.

The data presented in Table 5.1 showed that as the 'peak current' and 'pulse on time' increased, the value of surface roughness also increased. With an increase in

concentration of added powders, surface roughness decreased in both Al_2O_3 and SiC processes. However, among both the processes, SiC process gave better results than Al_2O_3 process.

Surface Roughness (Ra) Analysis (Cut off value = 2.5 and tracing = 5 mm)							
Parame-ters	Reverse Polarity Process						
	Simple	Al_2O_3 (Con.=2 g/l)	Al_2O_3 (Con.=8 g/l)	Al_2O_3 (Con.=16 g/l)	SiC (Con.=2 g/l)	SiC (Con.=8 g/l)	SiC (Con.=16 g/l)
Pc=4 Pon=4 Poff=6	21	24	20	16	24	13	7
Pc=4 Pon=5 Poff=6	30	27	26	23	22	16	17
Pc=5 Pon=4 Poff=6	29	28	20	22	28	19	18
Pc=5 Pon=5 Poff=6	31	19	21	19	19	19	18
Pc=6 Pon=4 Poff=6	33	25	22	24	24	21	20
Pc=6 Pon=5 Poff=6	34	25	24	25	24	24	23

Table 5.2: Showing different values of surface roughness for various parameters. Where Pc = Peak current in amp, Pon = Pulse on time, and Poff = Pulse off time.

The data presented in Table 5.2 showed that as the 'peak current' and 'pulse on time' increased, the value of surface roughness also increased. With an increase in concentration of added powders, surface roughness decreased in both Al_2O_3 and SiC processes. However, among both the processes, SiC process gave better results than Al_2O_3 process. While comparing the values of roughness presented in Tables 5.1 and 5.2, it was observed that the value of surface roughness (Ra) was lower in straight polarity process.

5.2 Calculation of MRR and TWR

MRR

The MRR of machined surface of each workpiece was calculated with weighing machine. It was calculated by taking weight of workpiece after every cut (machining). The formula used for this purpose was as given below:

MRR = Initial weight of workpiece before machining – Weight of workpiece after machining.

In this way, the weights of total of 84 cuts (machining) were taken.

After calculating MRR of each cut, the values of 6 cuts (machining) of one process were added to work out the final value of each process.

MRR values (g)							
Straight Polarity Process							
Different Parameters	Simple	Al_2O_3 (Con.=2 g/l)	Al_2O_3 (Con.=8 g/l)	Al_2O_3 (Con.=16 g/l)	SiC (Con.=2 g/l)	SiC (Con.=8 g/l)	SiC (Con.=16 g/l)
	19.43	19.40	19.30	19.40	17.90	17.87	17.55

Table 5.3: Showing different values of MRR for various parameters.

MRR values (g)							
Reverse Polarity Process							
Different Parameters	Simple	Al_2O_3 (Con.=2 g/l)	Al_2O_3 (Con.=8 g/l)	Al_2O_3 (Con.=16 g/l)	SiC (Con.=2 g/l)	SiC (Con.=8 g/l)	SiC (Con.=16 g/l)
	0.64	0.55	0.59	0.62	0.29	0.27	0.33

Table 5.4: Showing different values of MRR for various parameters.

The data presented in Tables 5.3 and 5.4 showed that MRR value was more in simple process as compared to Al_2O_3 and SiC processes. The value of MRR was more in Al_2O_3 process and this value was more than the SiC process. The higher value of MRR recorded in the simple might be attributed to non-addition of powders. It is also evident that the value of MRR gets decreased with the deposition of powders on the machined surface of the workpiece.

Tool Wear Rate (TWR)

TWR of the copper electrode was also calculated by using weighing machine.

The formula used for this purpose was as given below:

TWR = Initial weight of electrode before machining – Weight of electrode after machining.

After calculating TWR of each cut, the values of 6 cuts (machining) of each process were added to work out the final value of TWR.

TWR values (g)							
Straight Polarity Process							
Different Parameters	Simple	Al_2O_3 (Con.=2 g/l)	Al_2O_3 (Con.=8 g/l)	Al_2O_3 (Con.=16 g/l)	SiC (Con.=2 g/l)	SiC (Con.=8 g/l)	SiC (Con.=16 g/l)
	0.19	0.22	0.29	0.31	0.26	0.32	0.33

Table 5.5: Showing different values of MRR for various parameters.

TWR values (g)							
Reverse Polarity Process							
Different Parameters	Simple	Al_2O_3 (Con.=2 g/l)	Al_2O_3 (Con.=8 g/l)	Al_2O_3 (Con.=16 g/l)	SiC (Con.=2 g/l)	SiC (Con.=8 g/l)	SiC (Con.=16 g/l)
	0.07	0.06	0.06	0.06	0.03	0.03	0.03

Table 5.6: Showing different values of MRR for various parameters.

The data presented in Table 5.5 revealed that the TWR value in simple process under straight polarity was the lowest which could be ascribed to the accomplishment of the

process without deposition of powders while in other processes where powders were added, the TWR was higher in general but the highest in case of SiC when used at the concentration of 16 g/l. Perusal of the data presented in Table 5.6 indicated that inspite of the deposition of powders on the electrode, the TWR value did not get lowered in the reverse polarity process.

5.3 Hardness of Straight and Reverse Polarity Processes

Straight Polarity

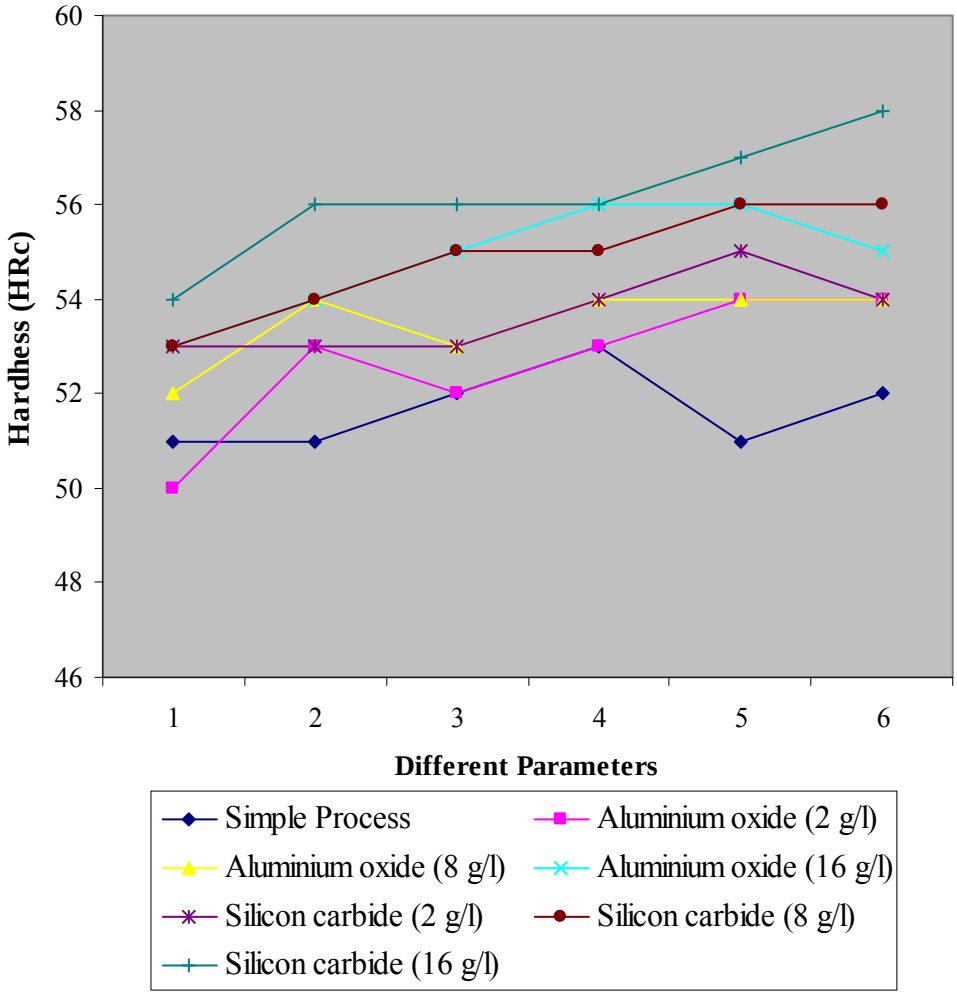

Figure 5.3: Showing hardness of straight polarity machined surfaces

Reverse Polarity

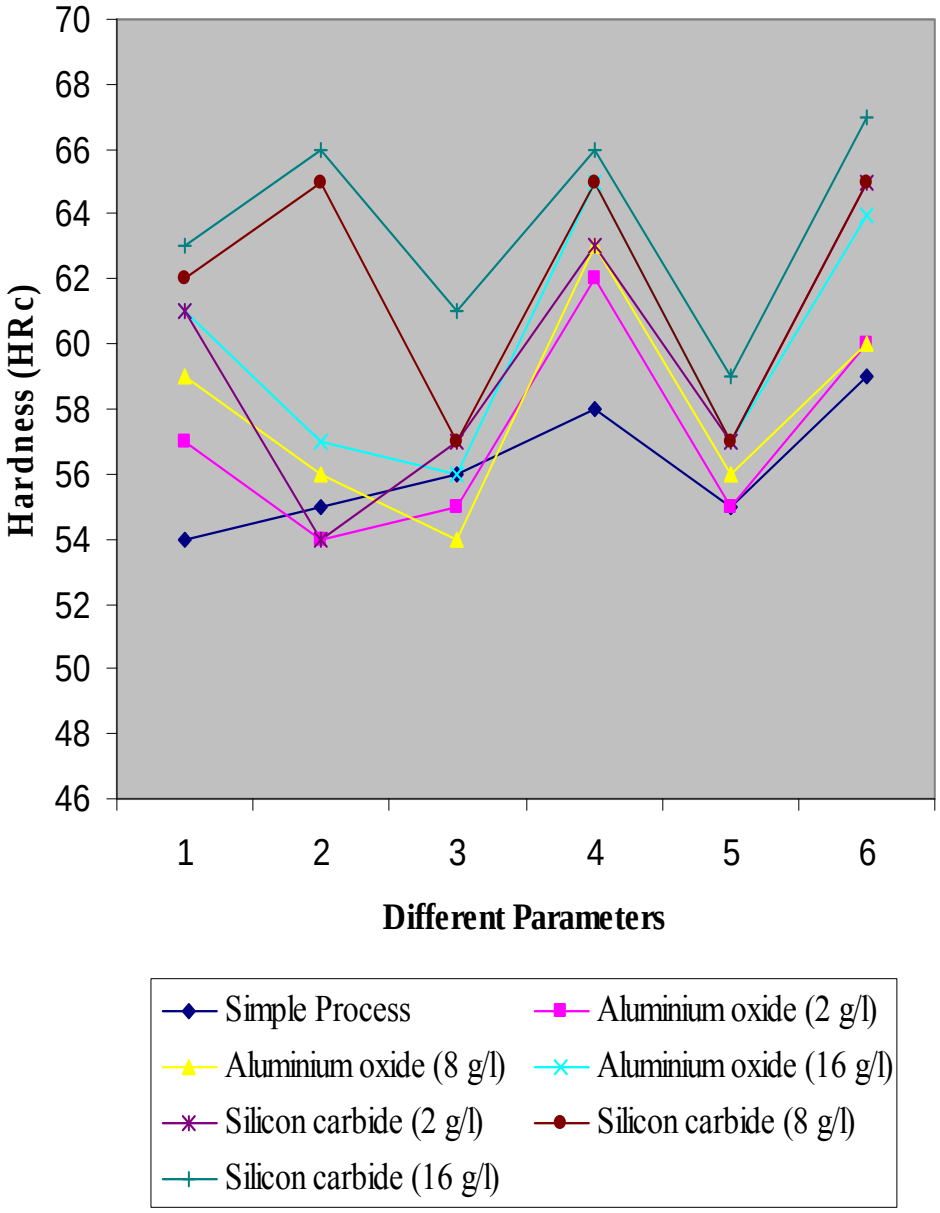

Figure 5.4: Showing hardness of reverse polarity machined surfaces.

Critical appraisal of the Figures 5.3 and 5.4 in respect of straight and reverse polarity respectively revealed that SiC @ 16 g/l imparted maximum hardness to the machined surface of the workpiece as compared with simple and Al_2O_3 processes.

5.4 SEM Analysis of Machined Surfaces

Scanning Electron Microscopy (SEM) of workpiece surfaces and powders was also measured to know the micro-structural changes which occurred.

Straight polarity machined surfaces

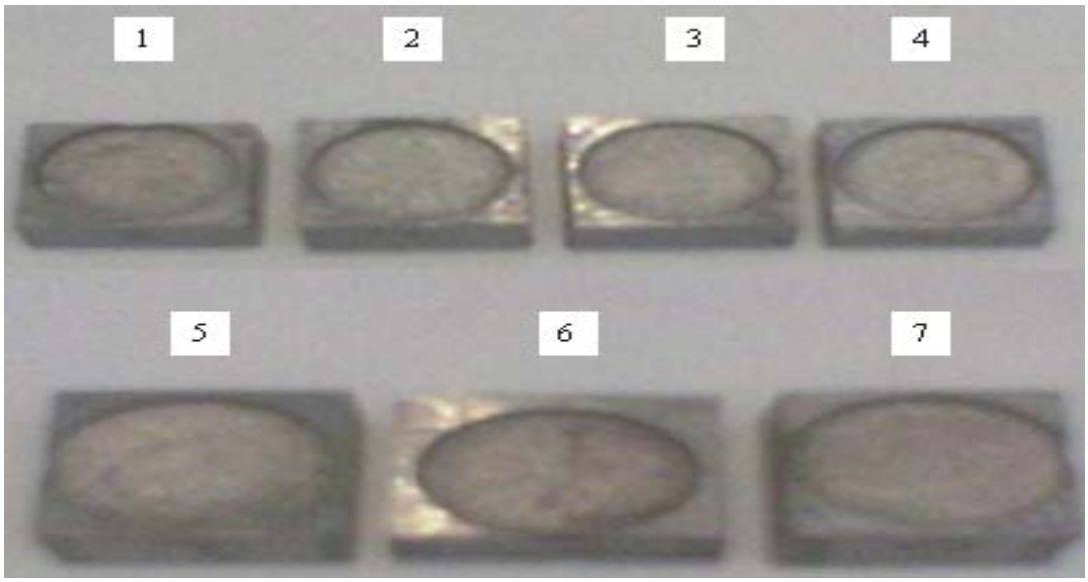

Figure 5.5: Showing straight polarity machined surfaces numbering 1 to 7.

1. Simple process machined surface with various parameters (Powder concentration = 0 g/l, Peak current = 4 amp, Pulse on time = 4 µs, and pulse off time = 6 µs).
2. Al_2O_3 process machined surface with various parameters (Powder concentration = 2 g/l, Peak current = 4 amp, Pulse on time = 4 µs, and pulse off time = 6 µs).
3. Al_2O_3 process machined surface with various parameters (Powder concentration = 8 g/l, Peak current = 4 amp, Pulse on time = 4 µs, and pulse off time = 6 µs).
4. Al_2O_3 process machined surface with various parameters (Powder concentration = 16 g/l, Peak current = 4 amp, Pulse on time = 4 µs, and pulse off time = 6 µs).

5. SiC process machined surface with various parameters (Powder concentration = 2 g/l, Peak current = 4 amp, Pulse on time = 4 µs, and pulse off time = 6 µs).
6. SiC process machined surface with various parameters (Powder concentration = 8 g/l, Peak current = 4 amp, Pulse on time = 4 µs, and pulse off time = 6 µs).
7. SiC process machined surface with various parameters (Powder concentration = 16 g/l, Peak current = 4 amp, Pulse on time = 4 µs, and pulse off time = 6 µs).

Reverse polarity machined surfaces

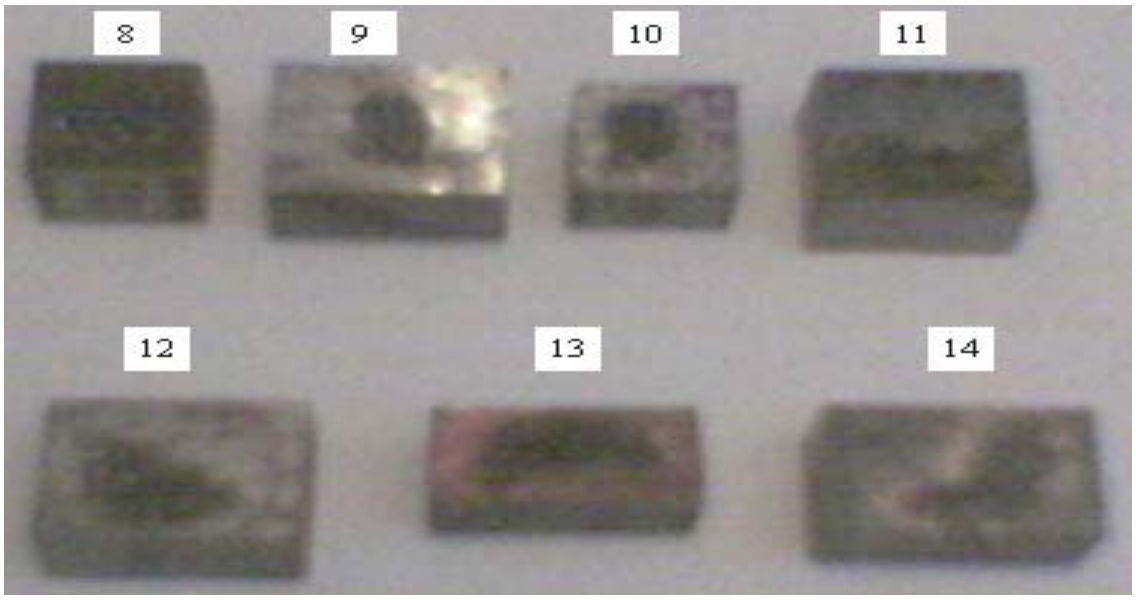

Figure 5.6: Showing reverse polarity machined surfaces numbering 8 to 14.

8. Simple process machined surface with various parameters (Powder concentration = o g/l, Peak current = 4 amp, Pulse on time = 4 µs, and pulse off time = 6 µs).
9. Al_2O_3 process machined surface with various parameters (Powder concentration = 2 g/l, Peak current = 4 amp, Pulse on time = 4 µs, and pulse off time = 6 µs).

10. Al_2O_3 process machined surface with various parameters (Powder concentration = 8 g/l, Peak current = 4 amp, Pulse on time = 4 µs, and pulse off time = 6 µs).
11. Al_2O_3 process machined surface with various parameters (Powder concentration = 16 g/l, Peak current = 4 amp, Pulse on time = 4 µs, and pulse off time = 6 µs).
12. SiC process machined surface with various parameters (Powder concentration = 2 g/l, Peak current = 4 amp, Pulse on time = 4 µs, and pulse off time = 6 µs).
13. SiC process machined surface with various parameters (Powder concentration = 8 g/l, Peak current = 4 amp, Pulse on time = 4 µs, and pulse off time = 6 µs).
14. SiC process machined surface with various parameters (Powder concentration = 16 g/l, Peak current = 4 amp, Pulse on time = 4 µs, and pulse off time = 6 µs).

The results obtained with/without use of powders of above machined surfaces numbering 1-14 are as given below:

1. Simple process machined surface with various parameters (Powder concentration = 0 g/l, Peak current = 4 amp, Pulse on time = 4 µs, and pulse off time = 6 µs).

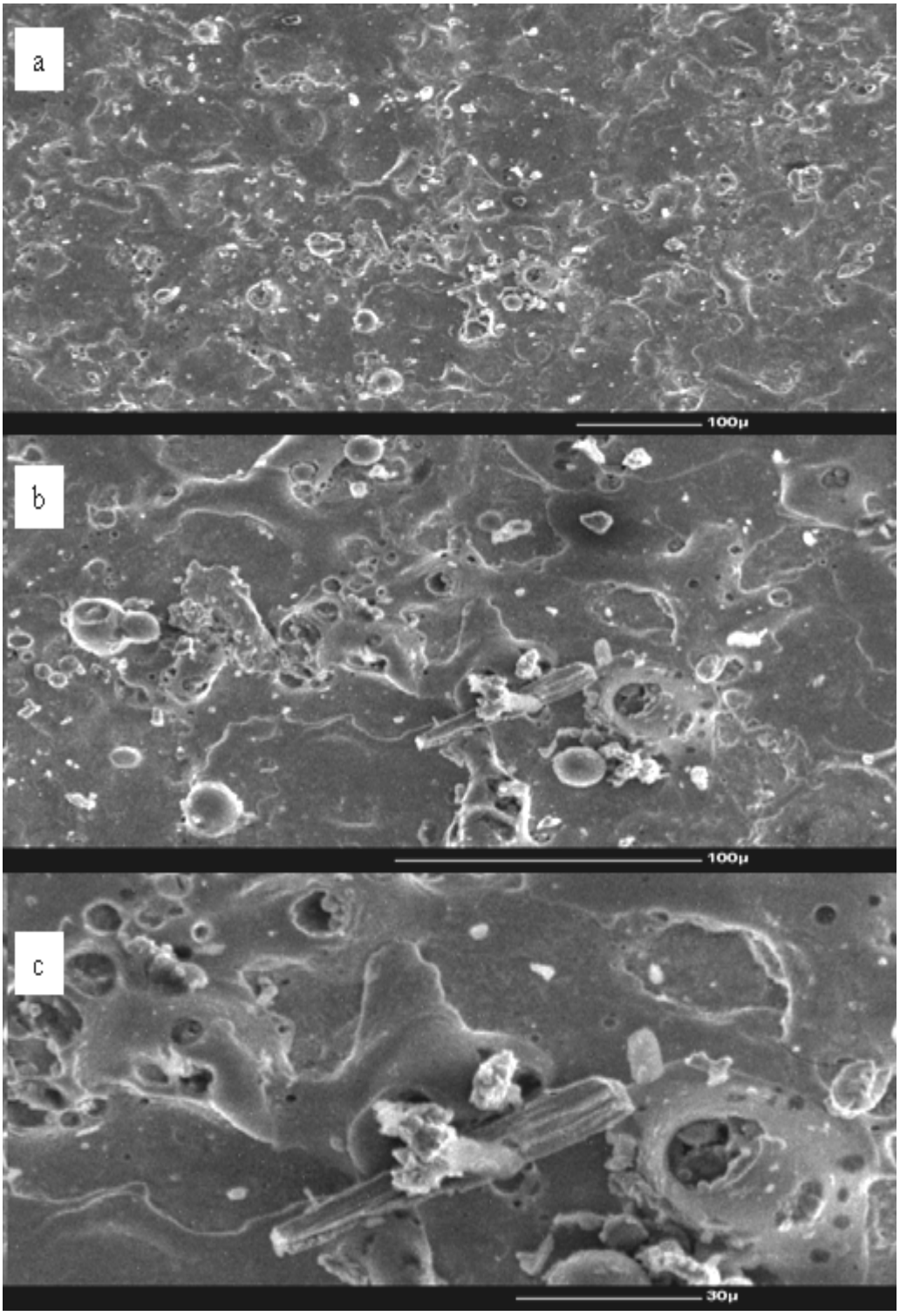

Figure 5.7: a) at 100 x, b) at 250 x, and c) at 500 x

2. Al_2O_3 process machined surface with various parameters (Powder concentration = 2 g/l, Peak current = 4 amp, Pulse on time = 4 µs, and pulse off time = 6 µs).

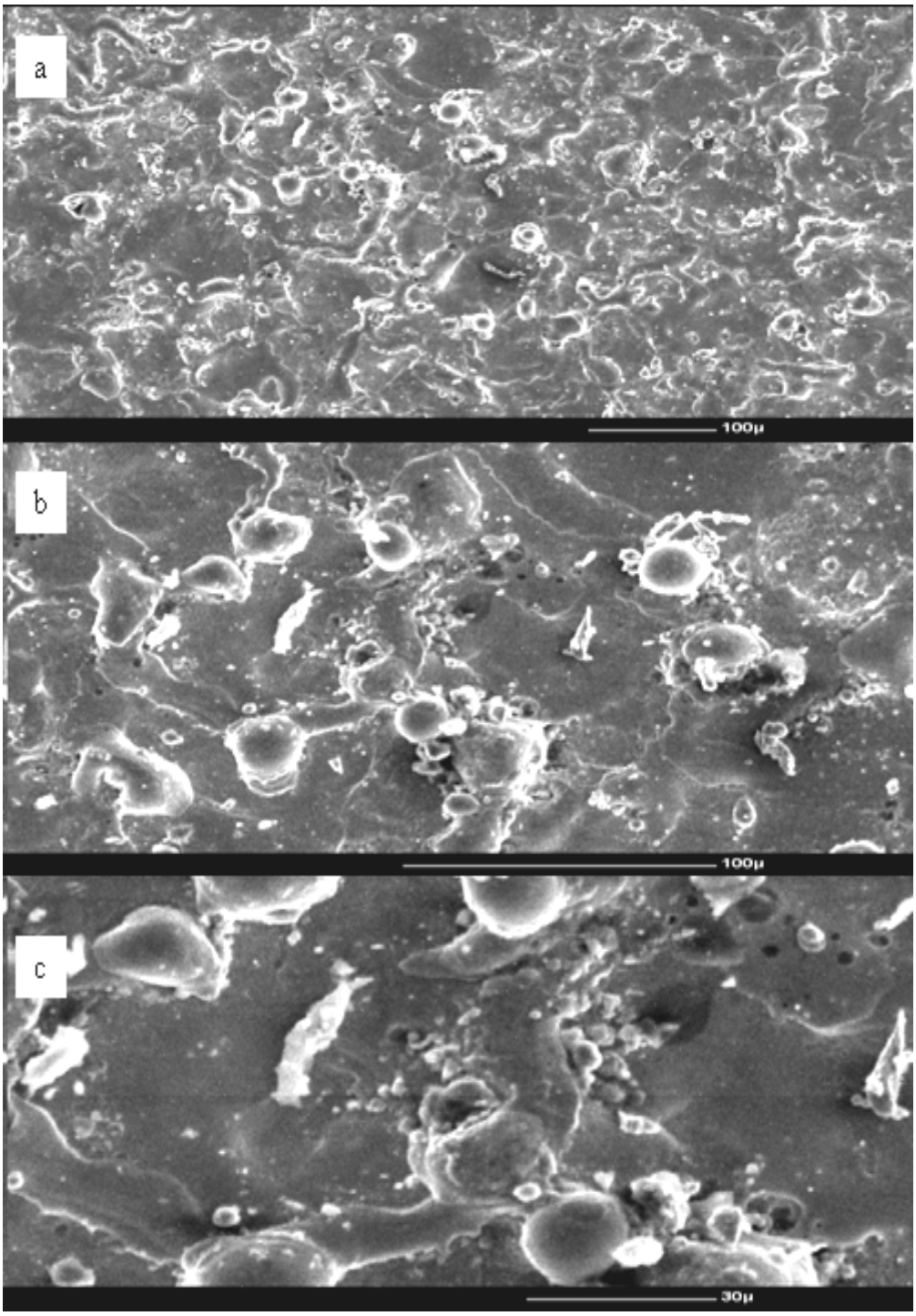

Figure 5.8: a) at 100 x, b) at 250 x, and c) at 500 x

3. Al_2O_3 process machined surface with various parameters (Powder concentration = 8 g/l, Peak current = 4 amp, Pulse on time = 4 µs, and pulse off time = 6 µs).

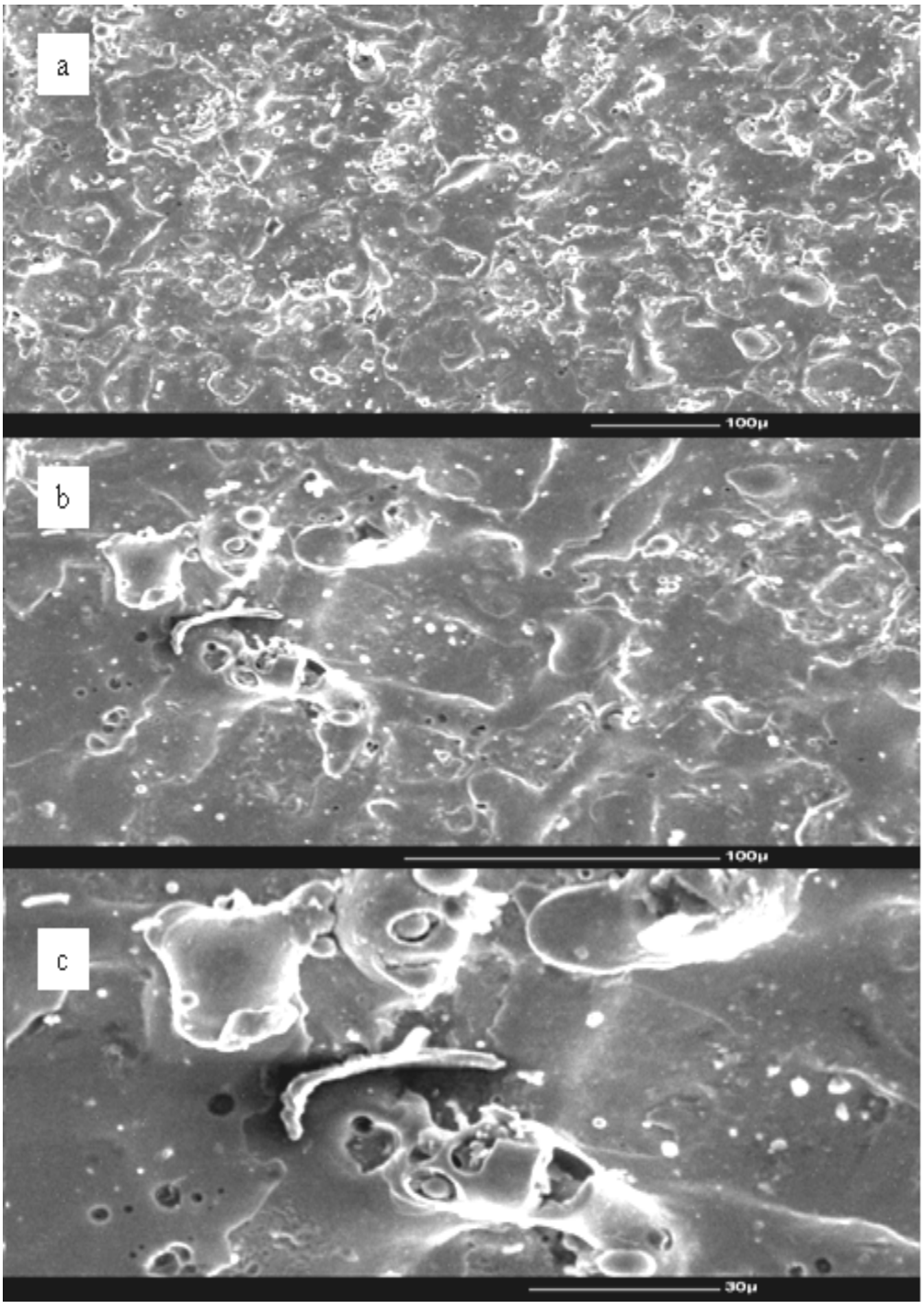

Figure 5.9: a) at 100 x, b) at 250 x, and c) at 500 x

4. Al_2O_3 process machined surface with various parameters (Powder concentration = 16 g/l, Peak current = 4 amp, Pulse on time = 4 µs, and pulse off time = 6 µs).

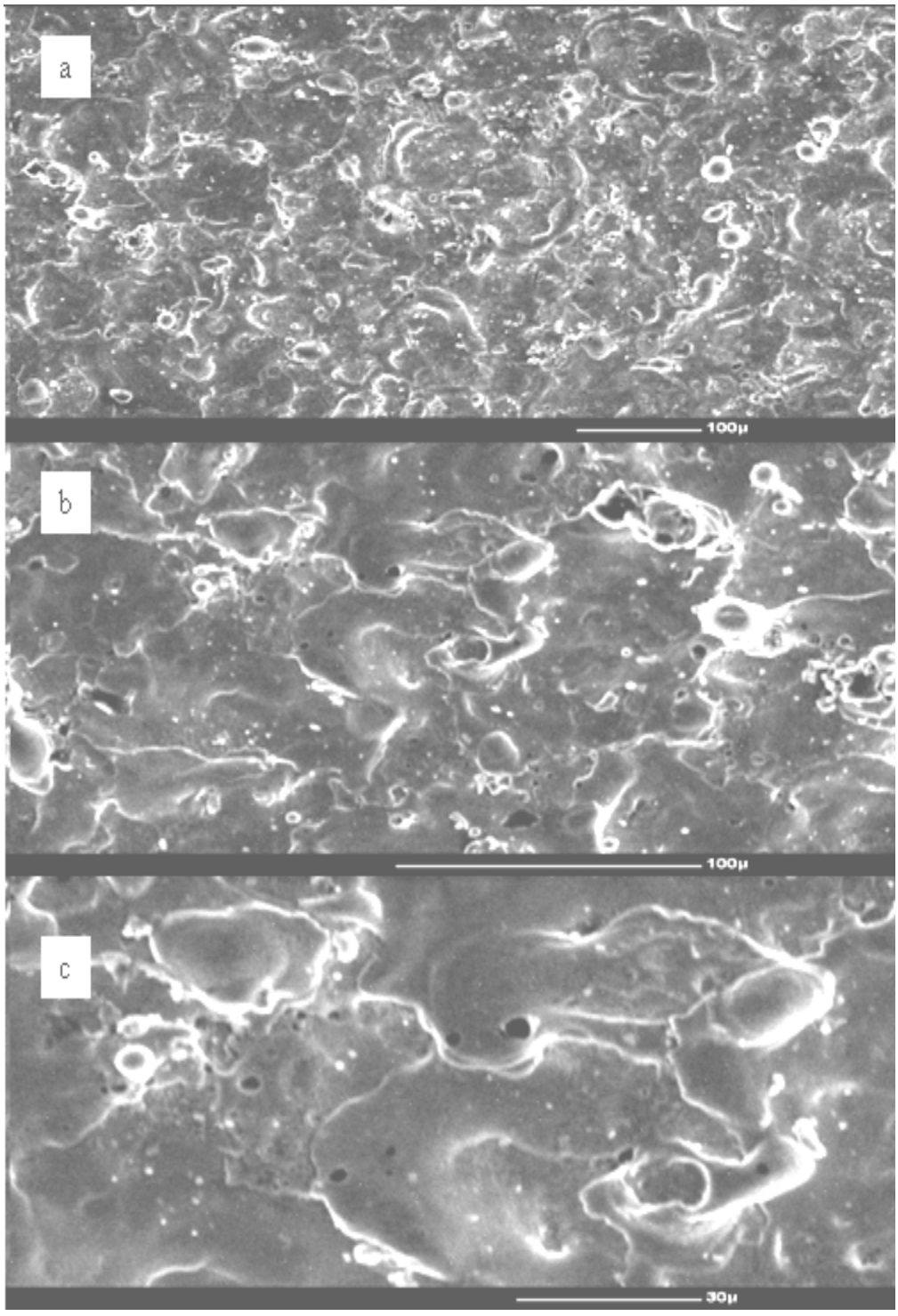

Figure 5.10: a) at 100 x, b) at 250 x, and c) at 500 x

5. SiC process machined surface with various parameters (Powder concentration = 2 g/l, Peak current = 4 amp, Pulse on time = 4 µs, and pulse off time = 6 µs).

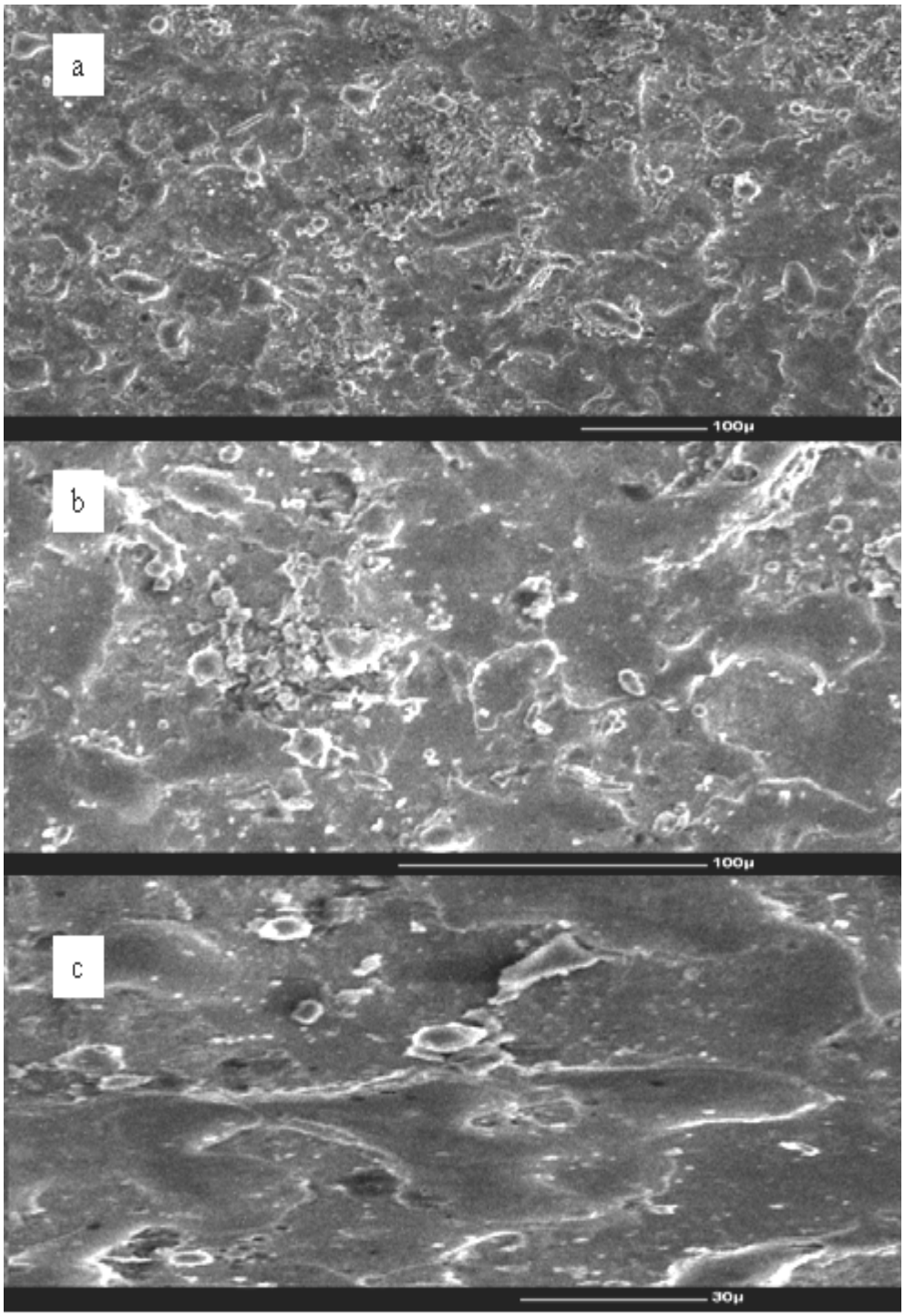

Figure 5.11: a) at 100 x, b) at 250 x, and c) at 500 x

6. SiC process machined surface with various parameters (Powder concentration = 8 g/l, Peak current = 4 amp, Pulse on time = 4 µs, and pulse off time = 6 µs).

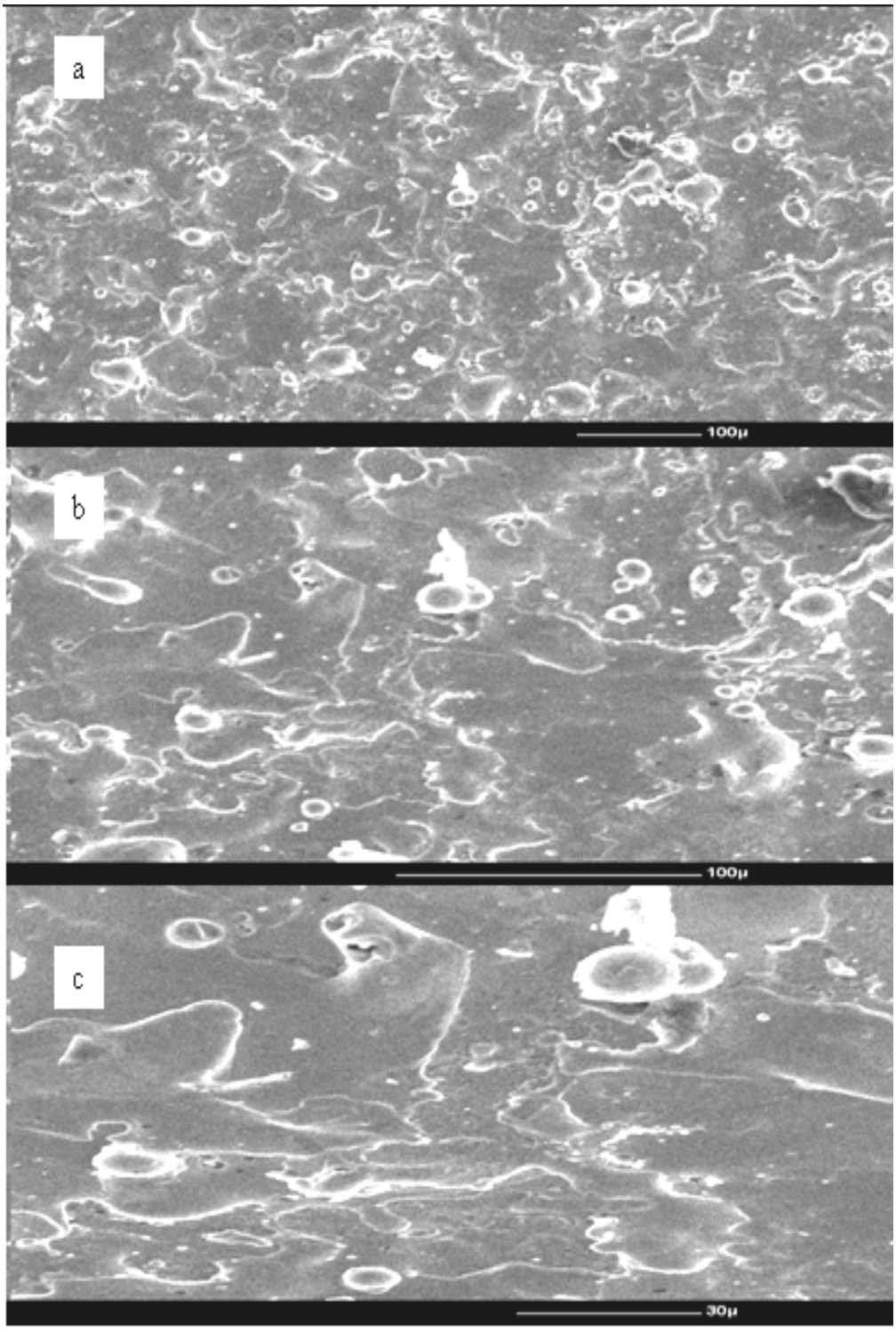

Figure 5.12: a) at 100 x, b) at 250 x, and c) at 500 x

7. SiC process machined surface with various parameters (Powder concentration = 16 g/l, Peak current = 4 amp, Pulse on time = 4 µs, and pulse off time = 6 µs).

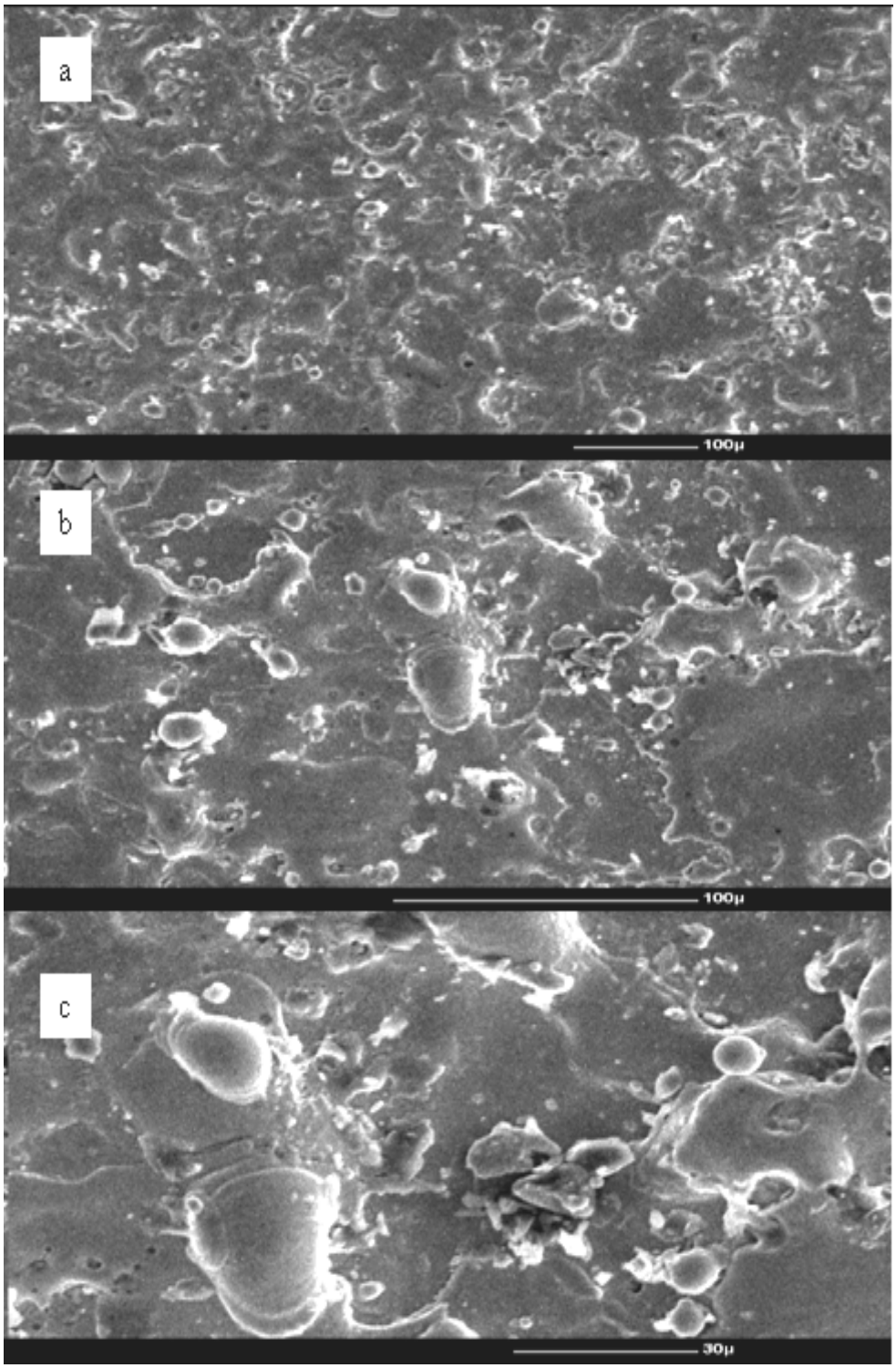

Figure 5.13: a) at 100 x, b) at 250 x, and c) at 500 x

8. Simple process machined surface with various parameters (Powder concentration = o g/l, Peak current = 4 amp, Pulse on time = 4 µs, and pulse off time = 6 µs).

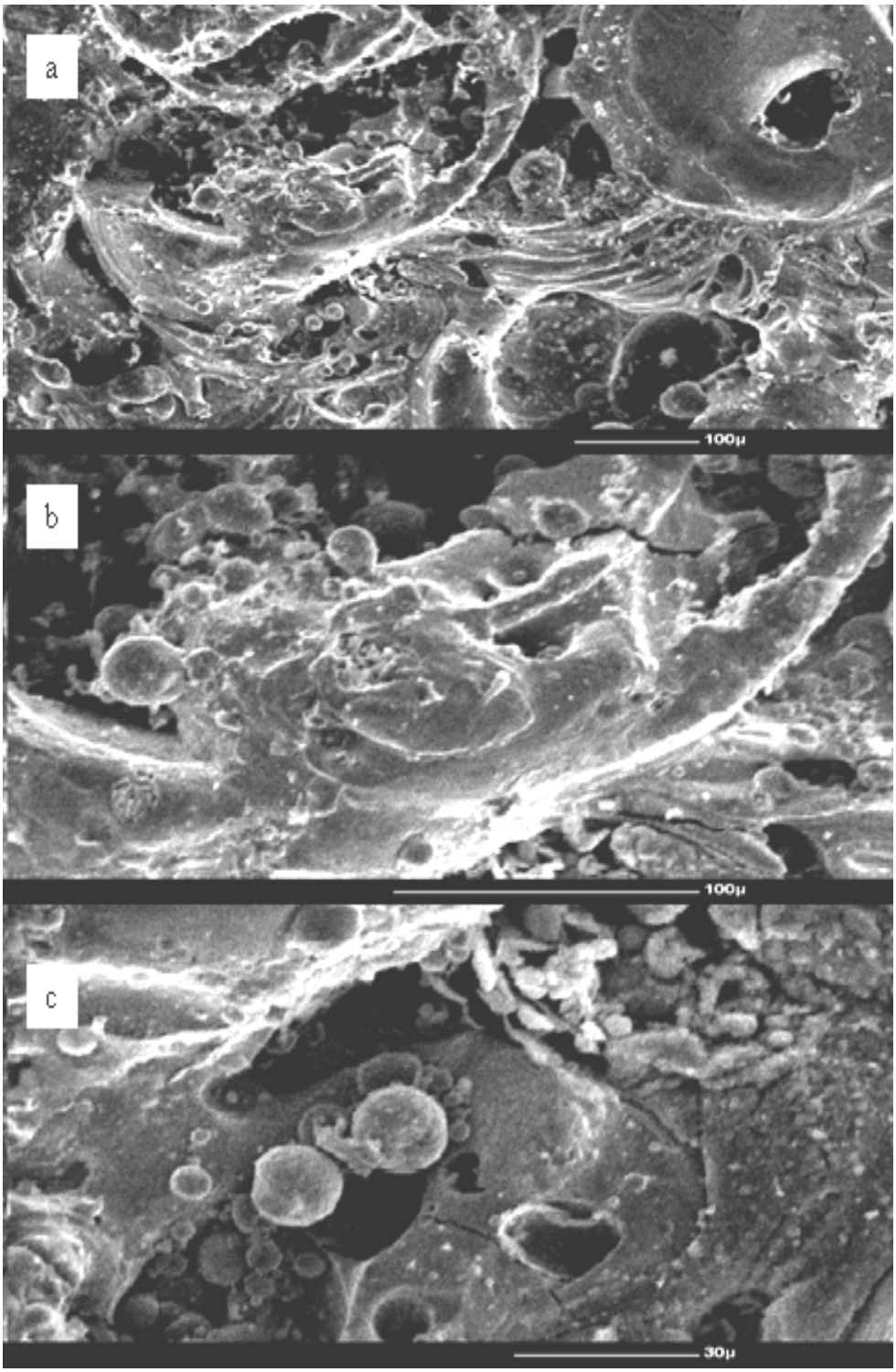

Figure 5.14: a) at 100 x, b) at 250 x, and c) at 500 x

9. Al_2O_3 process machined surface with various parameters (Powder concentration = 2 g/l, Peak current = 4 amp, Pulse on time = 4 µs, and pulse off time = 6 µs).

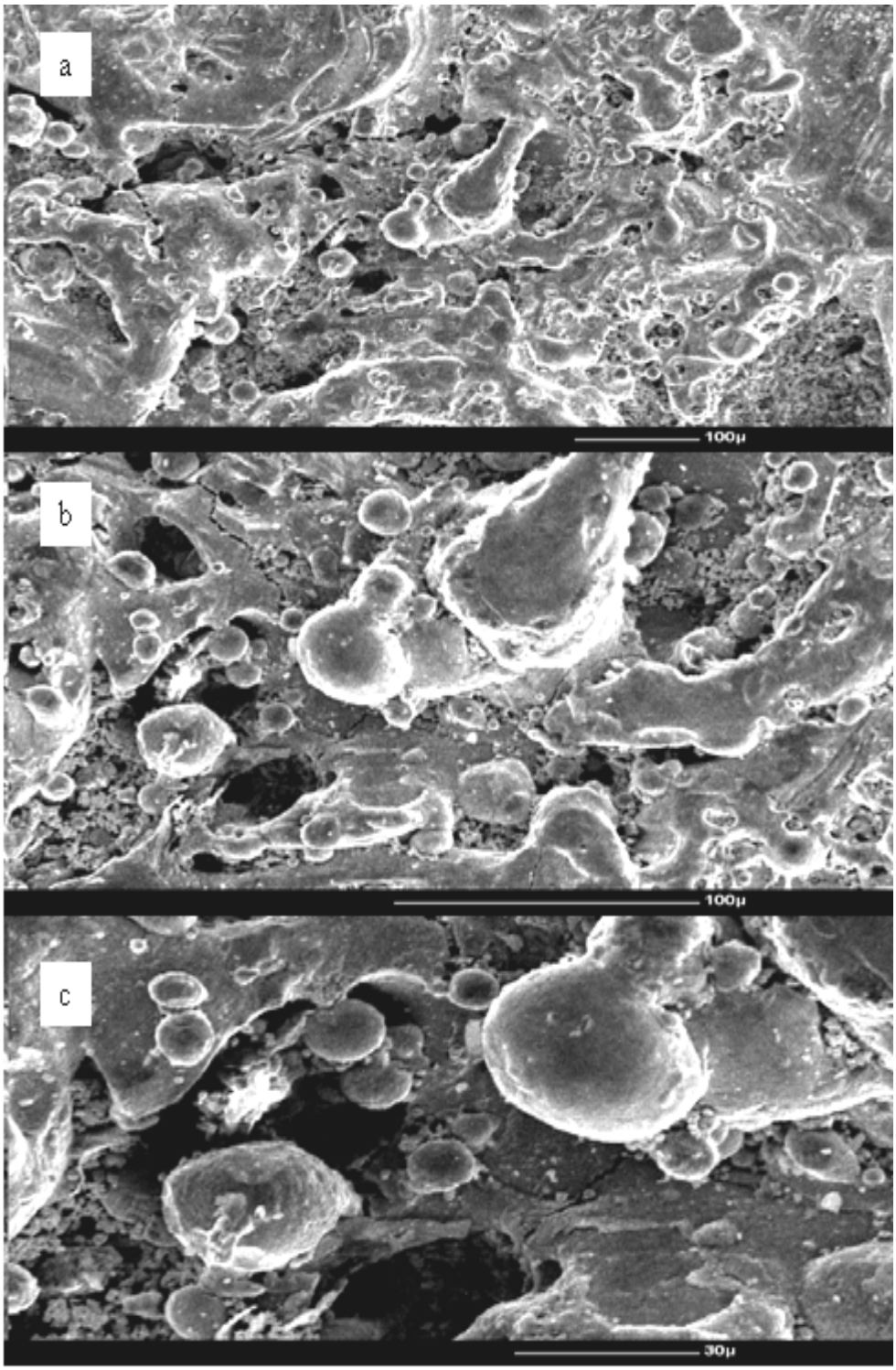

Figure 5.15: a) at 100 x, b) at 250 x, and c) at 500 x

10. Al_2O_3 process machined surface with various parameters (Powder concentration = 8 g/l, Peak current = 4 amp, Pulse on time = 4 µs, and pulse off time = 6 µs).

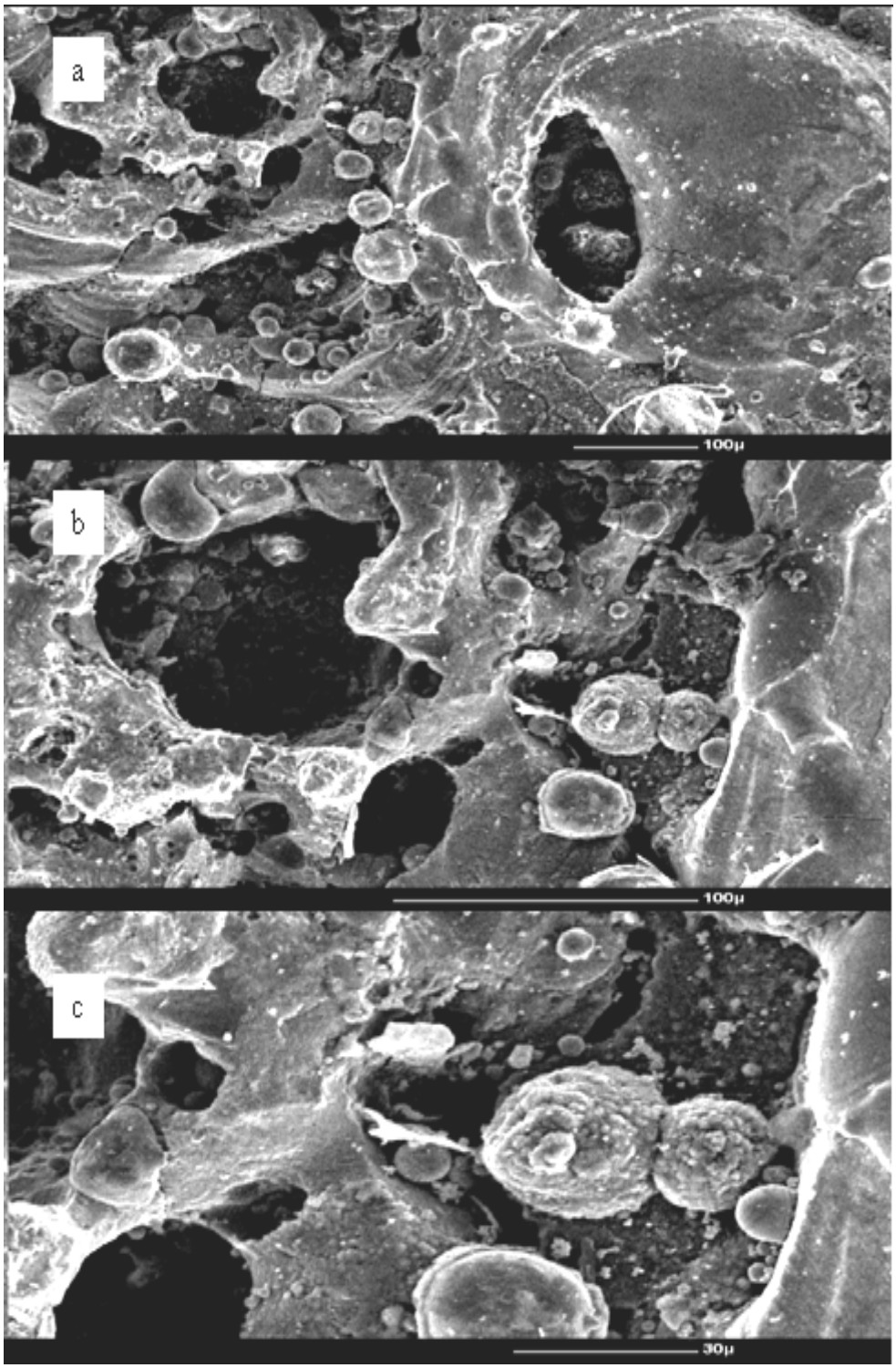

Figure 5.16: a) at 100 x, b) at 250 x, and c) at 500 x

11. Al_2O_3 process machined surface with various parameters (Powder concentration = 16 g/l, Peak current = 4 amp, Pulse on time = 4 µs, and pulse off time = 6 µs).

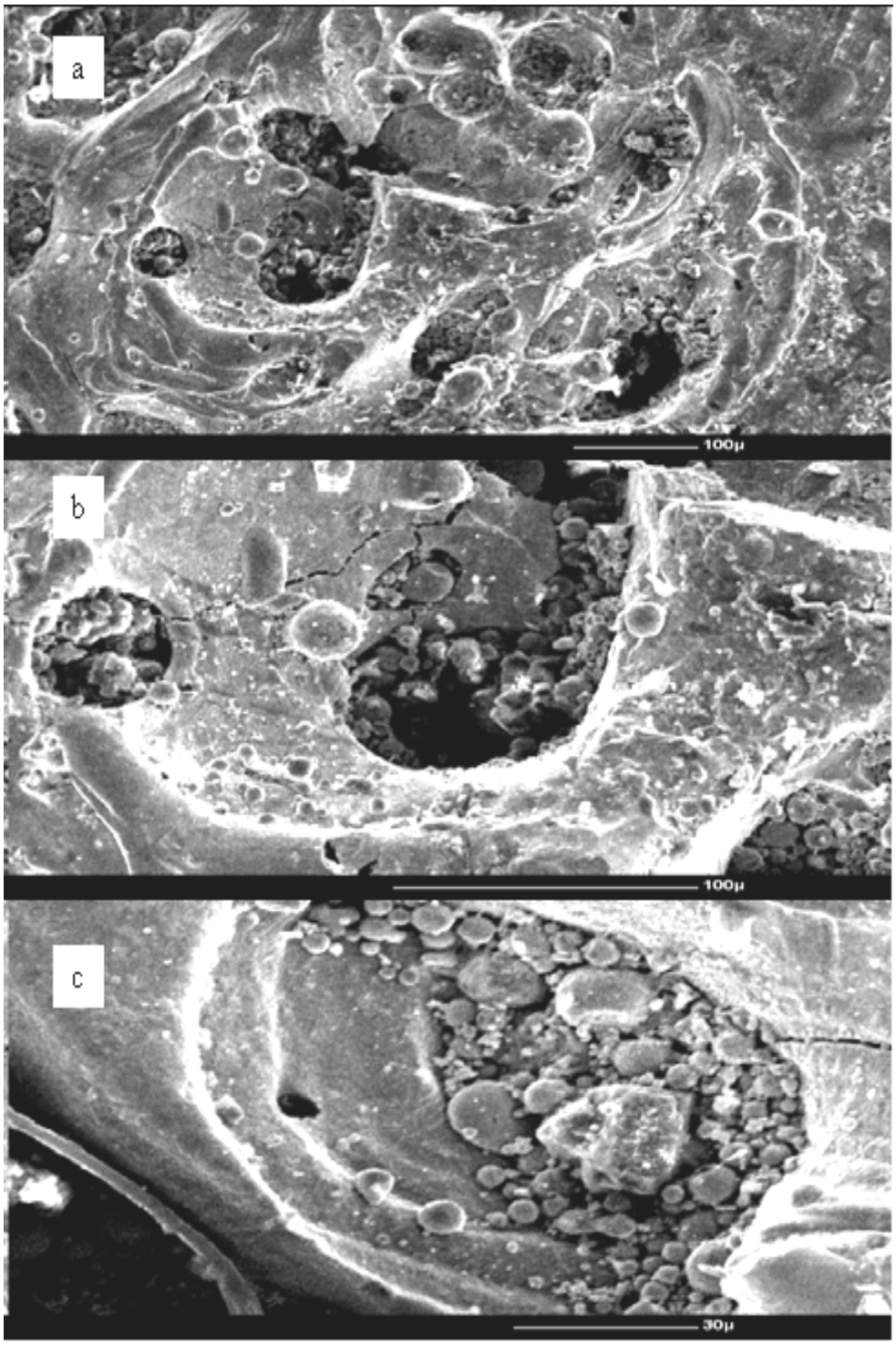

Figure 5.17: a) at 100 x, b) at 250 x, and c) at 500 x

12. SiC process machined surface with various parameters (Powder concentration = 2 g/l, Peak current = 4 amp, Pulse on time = 4 µs, and pulse off time = 6 µs).

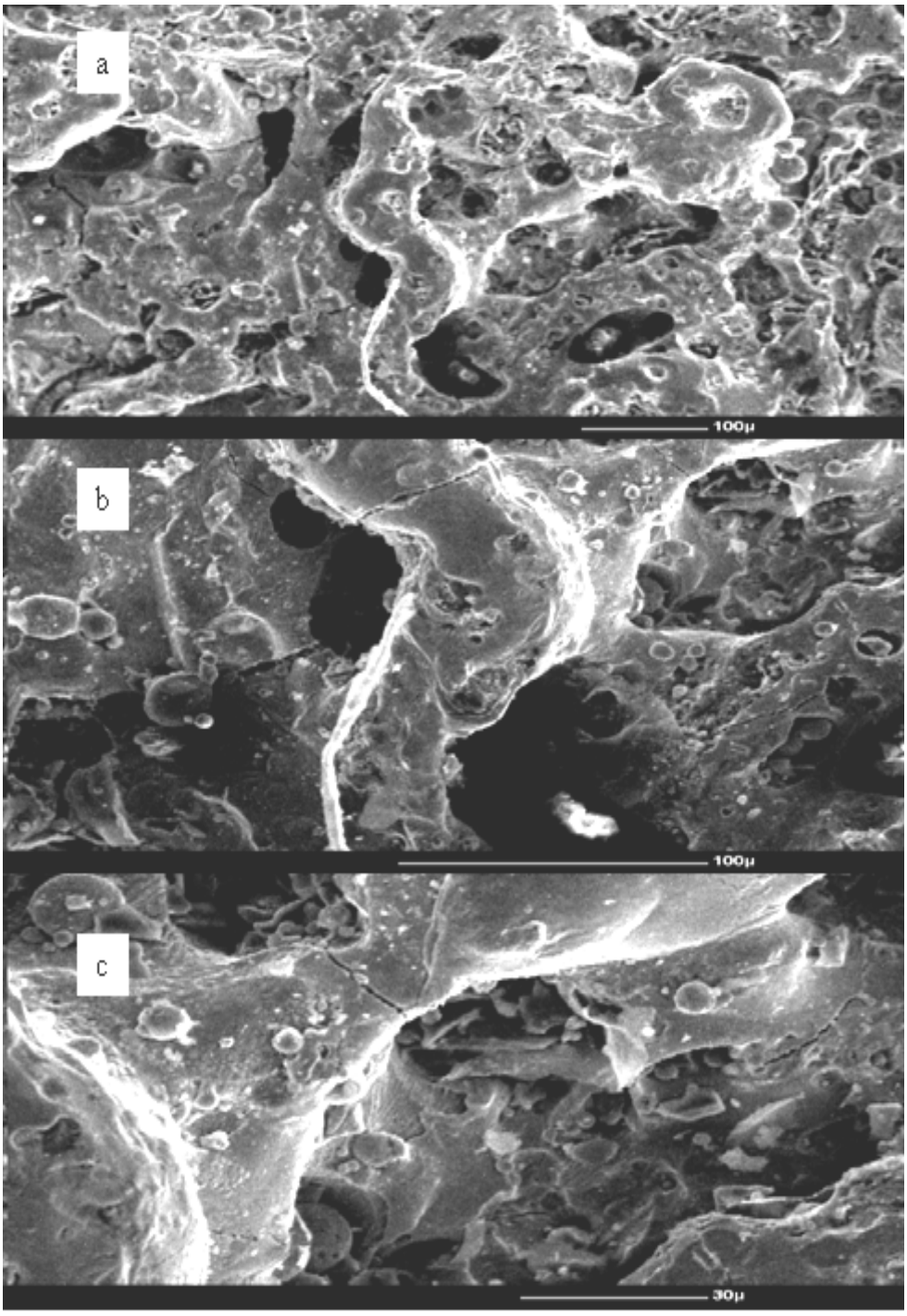

Figure 5.18: a) at 100 x, b) at 250 x, and c) at 500 x

13. SiC process machined surface with various parameters (Powder concentration = 8 g/l, Peak current = 4 amp, Pulse on time = 4 µs, and pulse off time = 6 µs).

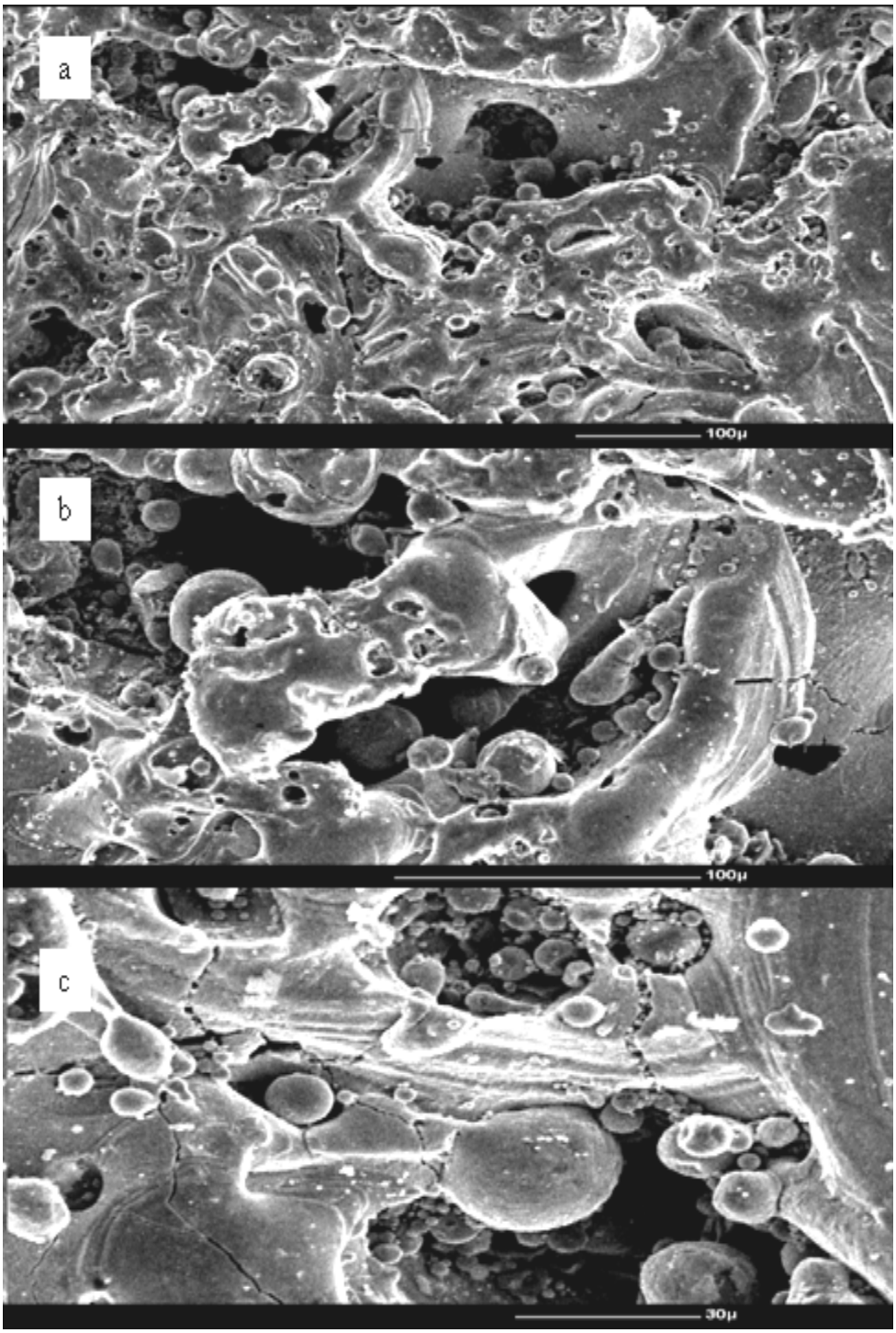

Figure 5.19: a) at 100 x, b) at 250 x, and c) at 500 x

14. SiC process machined surface with various parameters (Powder concentration = 16 g/l, Peak current = 4 amp, Pulse on time = 4 µs, and pulse off time = 6 µs).

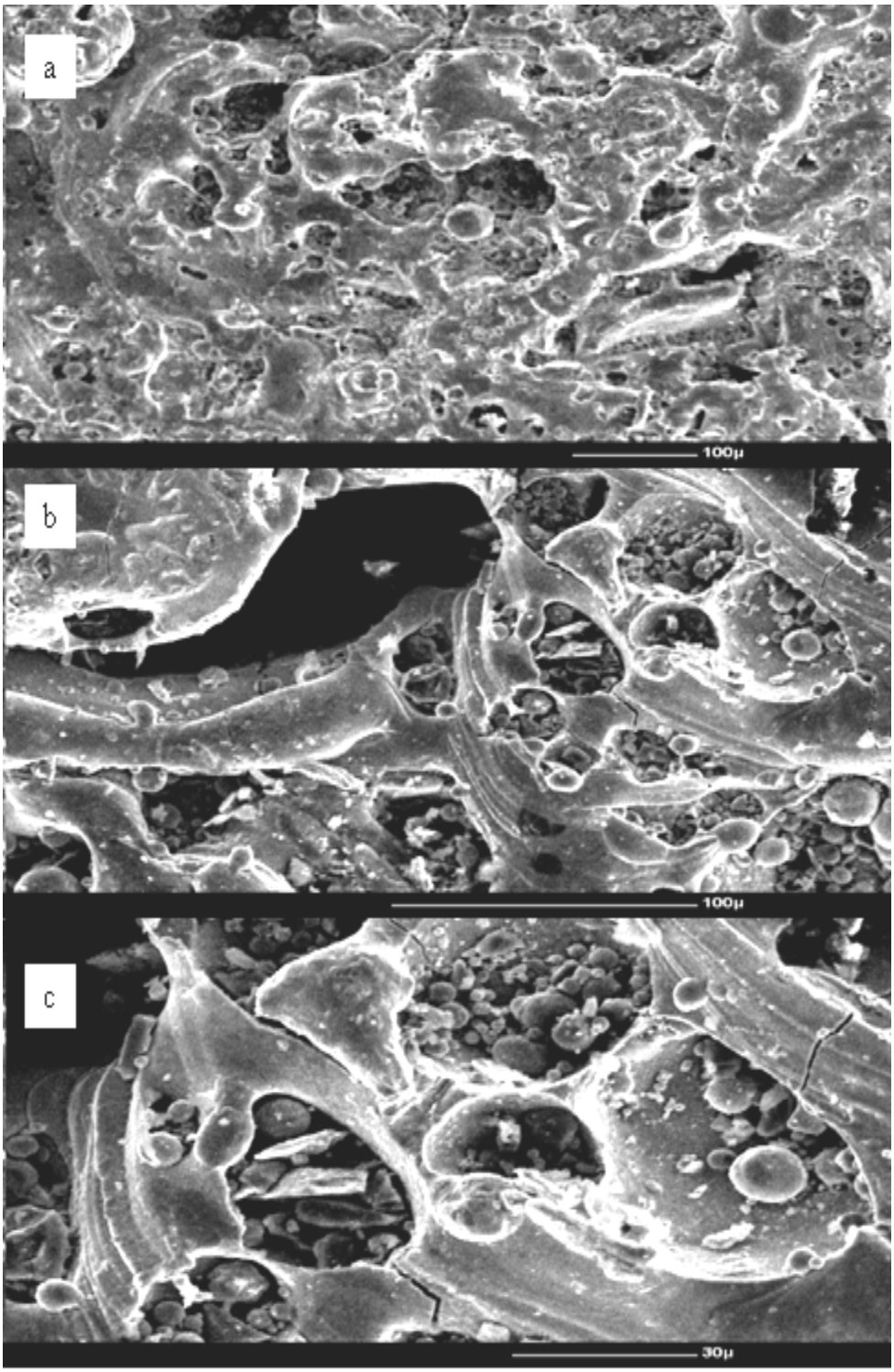

Figure 5.20: a) at 100 x, b) at 250 x, and c) at 500 x

Comparative study of the Figures 5.7-5.20 revealed that as the concentration of powders increased, the sizes and depths of cavities and dark holes were decreased in the machined surface. Such effects were recorded to be more prominent in the SiC process when powder was used @ 16 g/l.

Chapter-6
Conclusions and Scope

Based on the investigations carried out on the research problem, the following points could be concluded:

1. Addition of Al_2O_3 active neutral and SiC powders reduced the SR as compared to simple EDM process. But SiC powder reduced roughness remarkably as compared to Al_2O_3 powder.
2. Addition of SiC powder increased the hardness of the machined surface more than the Al_2O_3 machined surface. SiC @ 16 g/l gave the highest values of hardness.
3. Scanning Electron Microscope (SEM) study of PMEDM process showed that the cavities produced were shallow and uniform.
4. MRR of workpiece was more in straight polarity process than reverse polarity process.
5. TWR value in simple process under straight polarity was the lowest. The TWR was lower in Al_2O_3 process.

The above results could find their application in the industry. There is a great scope of future work that can be taken up for further refinement of PMEDM process. A few of the areas may me mentioned as below:

1. In PMEDM process, material removal process takes place because of spark produced between the electrode and the workpiece, and a lot of energy is generated. This energy causes rise in temperature. There is variation in temperature during the process of machining. This variation in temperature can be further ascertained.
2. Since a number of parameters affect performance of PMEDM process, mathematical models may be developed to determine the effect of each parameter.
3. The experimental study has been made using Al_2O_3 active neutral and SiC powders into dielectric fluid. Various parameters need to be studied by using mixture of these and other powders.

References

Chang, Yih-Fang (2005). Mixed $H_2/H\infty$ optimization approach to gap control on EDM. *Control Engg. Practice*, **13,** 95-104.

Chang, Y.F. and Chiu, Z.H. (2004). Electrode wear-compensation of electric discharge scanning process using a robust gap-control. *Mechatronics*, **14**, 1121-39.

Chang, Yih-Fang and Hong, Rong-Chi (2005). Parametric curve machining of a CNC milling EDM. *Int. J. Mach. Tools Manuf.*, **45** , 941-948.

Chen, Y. and Mahdavian, S.M. (1999). Parametric study into erosion wear in a computer numerical controlled electro-discharge machining process. *Wear*, **236,** 350-354.

Ekmekci, B., Tekkaya, A.E. and Erden, A. (2005). A semi empirical approach for residual stresses in electric discharge machining (EDM). *Int. J. Mach. Tools Manuf.,* **20,** 1-11.

Furutani, K., Saneto, A., Takezawa, H., Mohri, N. and Miyake, H. (2001). Accretion of titanium carbide by electrical discharge machinery with powder suspended in working fluid. *J. Int. Soc. Precision Engg. Nanotechnology*, **25,** 138-144.

Ghoreishi, M. and Atkinson, J. (2002). A comparative experimental study of machining characteristics in vibratory, rotary and vibro-rotary electro-discharge machining. *J. Mater. Procc. Technol*., **120**, 374-384.

Han, F. and Kunieda, M. (2004). Development of parallel electrical discharge machining. *Precision Engg.,* **28**, 65-72.

Han, F., Wachi, S. and Kunienda, M. (2004). Improvement of machining characteristics of micro-EDM using transistor type isopulse generator and servo feed control. *Precision Engg.,* **28**, 378-85.

Ho, K.H., Newman, S.T., Rahimifard, S. and Allen, R.D. (2004). State of the art in wire electrical discharge machining (WEDM). *Int. J. Mach. Tools Manuf.*, **44,** 1247-1259.

Hsue, W. J., Liao, Y. S. and Lu., S.S. (1999). Fundamental geometry analysis of wire electric discharge machining in corner cutting. *Int. J. Meach. Tools Manuf.,* **39**, 651-667.

Hu, A.M. and Dean T.A. (2000). A study of surface topography, friction and lubricants in metalforming. *Int. J. Mach. Tools Manuf.*, **40,** 1637-1649.

Jain, R.K. (1995). Production Technology. Khanna Publishers, Delhi. pp 432-433

Janousek, L., Chen, Z., Yusa, N. and Miya, K. (2005). Excitation with phase shifted fields-enhancing evaluation of deep cracks in eddy-current testing. *NDT&E Int.* **38,** 508-515.

Kawaoka H. Kim, Y. H., Sekino, T., Choa, Y. H., Kusunose, T., Nakayama, T. and Niihara, K. (2001). New approach to provide an electrical conductivity to structural ceramics. *J. Ceram. Procc. Res.,* **2**, 1-3.

Ker, M.D. (1998). Electrostatic discharge (ESD) protection for CMOS output buffers in scaled-down VLSI technology. *Microelectron. Reliab.,* **38**, 619-639.

Klocke, F., Lung, D., Antonoglou, G. and Thomaidis, D. (2004). The effects of powder suspended dielectrics on the thermal influenced zone by electrodischarge machining with small discharge energies. *J. Mater. Process. Technol.,* **149**, 191-197.

Kunieda, M. and Ojima, S. (2000). Improvement of EDM efficiency of silicon single crytal through ohmic contact. *J. Int. Soc. Precision Engg. Nanotechnology* **24,** 185-190.

Liu, H.S., Yan, B.H., Chen, C.L. and Huang, F.Y. (2005). Application of micro-EDM combined with high-frequency dither grinding to micro-hole machining. *Int. J. Mach. Tools Manuf.*, **20,** 1-8.

Marafona, J. and Chousal, J.A.G. (2005). A finite element model of EDM based on the Joule effect. *Int. J. Mach. Tools Manuf.*, **20,** 1-8.

Miller, S.F., Kao, Chen-C, Shih, A.J. and Qu, J. (2005). Investigation of wire electrical discharge machining of thin cross-sections and compliant mechanisms. *Int. J. Mach. Tools Manuf.*, **45,** 1717-1725.

Moro. T., Mohri, N., Otsubo, H., Goto, A. and Saito, N. (2004). Study on the surface modification system with electric discharge machine in the paractical usuage. J. Mater. Process. Technol. **149**, 65-70.

Park, J.H.P., Koh, Y.H., Kim, H.E. and Hwang, C.S. (1999). Densification and mechanical properties of titanium diboride with with silicon nitride as a sintering aid. J. Am. Ceram. Soc., **82**, 3037-3042.

Pecas, P. and Henriques, E. (2003). Influence of silicon powder-mixing dielectric on conventional electrical discharge machining. *Int. J. Mach. Tools Manuf.*, **43,** 1465-1471.

Pham, D.T., Dimov, S.S., Bigot, S., Ivanov, A. and Popov, K. (2004). Micro-EDM-recent developments and research issues. J. Mater. Process. Technol. **149**, 50-57.

Puri, A.B. and Bhattacharyya, B. (2003). An analysis and optimization of the geometrical inaccuracy due to wire lag phenomenon in WEDM. Int. J. Mach. Tools Manuf., **43**, 151-159.

Ramasawmy, H., Blunt, L. and Rajurkar, K.P. (2005). Investigation of the relationship between the white layer thickness and 3D surface texture parameters in the die sinking EDM process. *Precision Engg.,* **29**, 479-490.

Rehbein,W., Schlze, H.P., Mecke, K., Wollonberg, G. and Storr, M. (2004). Influence of selected groups of additives on breakdown in EDM sinking. *J. Mater. Procc. Technol.*, **149**, 58-64.

Sanchez, J. A., Lopez de Lacalle, L.N., Lamikiz, A. and Bravo, U. (2002). Dimensional accuracy optimization of multi-stage planetary EDM. *Int. J. Mach. Tools Manuf.*, **42**, 1643-1648.

Simao, J., Lee, H.G., Aspinwall, D.K., Dewes, R.C. and Aspinwall, E.M. (2003). Workpiece surface modification using electrical discharge machining. *Int. J. Mach. Tools Manuf.,* **43,** 121-128.

Stampfi, J., Leitgeb, R., Cheng Y. L. and Prinz F. B. (2000). Electro-discharge machining of microscopic parts with electroplated copper and hot-pressed silver tungsten electrodes. *J. Micromech. Microeng.,* **10**, 1-6.

Wang, J. and Ravani, B. (2003). Computer aided contouring operation for traveling wire electric discharge machining (EDM). *Comput. Aid. Des.,* **35**, 925-934.

Wu, K.L., Yan, B.H., Huang, F.Y. and Chen, S.C. (2005). Improvement of surface finish on SKD steel using electro-discharge machining with alminium and surfactant added dielectric. *Int. J. Mach. Tools Manuf.,* **45,** 1195-1201.

Yan, B.H., Lin, Y.C. and Huang, F.Y. (2002). Surface modification of Al-Zn-Mg alloy by combined electrical discharge machining with ball burnish machining. *Int. J. Mach. Tools Manuf.*, **42,** 925-934.

Zhixin, J. Xing, A. and Jianhua, Z. (1995). Study on mechanical pulse electric discharge machining. *Precision Engg.*, **17**, 89-93.